THE UNIVERSITY OF MICHIGAN

INDUSTRY PROGRAM OF THE COLLEGE OF ENGINEERING

STRESSES IN RING STIFFENERS IN CYLINDERS SUBJECTED TO BENDING

W. S. Rumman

May, 1961

IP-514

TABLE OF CONTENTS

LIST OF TABLES

LIST OF FIGURES

LIST OF FIGURES (CONT'D)

INTRODUCTION

A considerable amount of experimental and theoretical work has been made by various investigators[1,2,3] on the ultimate capacity of thin-walled cylinders both stiffened and unstiffened. However, very little has been done to determine the nature and magnitude of the forces acting on ring stiffeners in thin-walled cylinders subjected to bending.

Ring stiffeners are used in steel chimneys and in many pipe and conduit structures. Although the rigidity of the stiffener is an important factor in its selection, the designer, nevertheless, needs to determine the nature and magnitude of the forces to which the stiffener is subjected. Therefore, this investigation is primarily concerned with establishing a practical approach for determining the distribution and magnitude of the forces acting on ring stiffeners in cylinders subjected to bending. Only cylinders with constant radius and thickness and with equidistant stiffeners are considered.

Notation - The letter symbols adopted for use in this paper are defined where they first appear, in the illustrations or in the text, and are arranged alphabetically, for convenience of reference, in the Appendix.

---

1 Brazier, L. G. "The Flexure of Thin Cylindrical Shells and Other 'Thin' Sections." Reports and Memoranda No. 1081, London: Aeronautical Research Committee, 1926.

2 Lundguist, Eugene E. "Strength Tests of Thin-Walled Duralumin Cylinders in Pure Bending." T.N. No. 479, NACA, 1933.

3 Peterson, James P. "Bending Tests of Ring-Stiffened Circular Cylinders." T.N. No. 3755, NACA, 1956.

THE SCOPE OF THE EXPERIMENTAL WORK

The objective of the experimental work was to measure the variations of the stresses on the stiffener as a result of the bending of the cylinder. A model (Figure 1) was therefore built which was essentially a thin-walled long cylinder of constant thickness and radius, and reinforced by equidistant circular rings. The material used in the fabrication of the model was aluminum alloy 6061-T6.

The circular cylinder was composed of three segments each equal to four feet in length. Each segment was rolled into its circular shape from a 0.025 inch thick sheet to a mean diameter of about 11.28 inches. The radius/thickness ratio of the model was therefore equal to 225.

The stiffeners were rolled from bars that were cut from a 0.25 inch thick plate. The bars were machined to the specified thickness of the stiffeners and were rolled to the right diameter. In each stiffener an allowance was made for a splice.

The end segments of the model were reinforced by 1/4" x 1/4" stiffeners spaced equally at 6 inches center to center. No strain gages were mounted on the end segments and no change in the size or spacing of their stiffeners was made during the test.

On the center segment, which is the actual test specimen of the model, two different size stiffeners were used during the test, 1/4" x 3/16" (width x thickness) and 1/4" x 1/8". For each of the two sizes, the stiffeners were originally spaced at 2-5/8" with provisions to remove some of the stiffeners during the test so that the spacing could be increased to 5-1/4", 10-1/2" and 21".

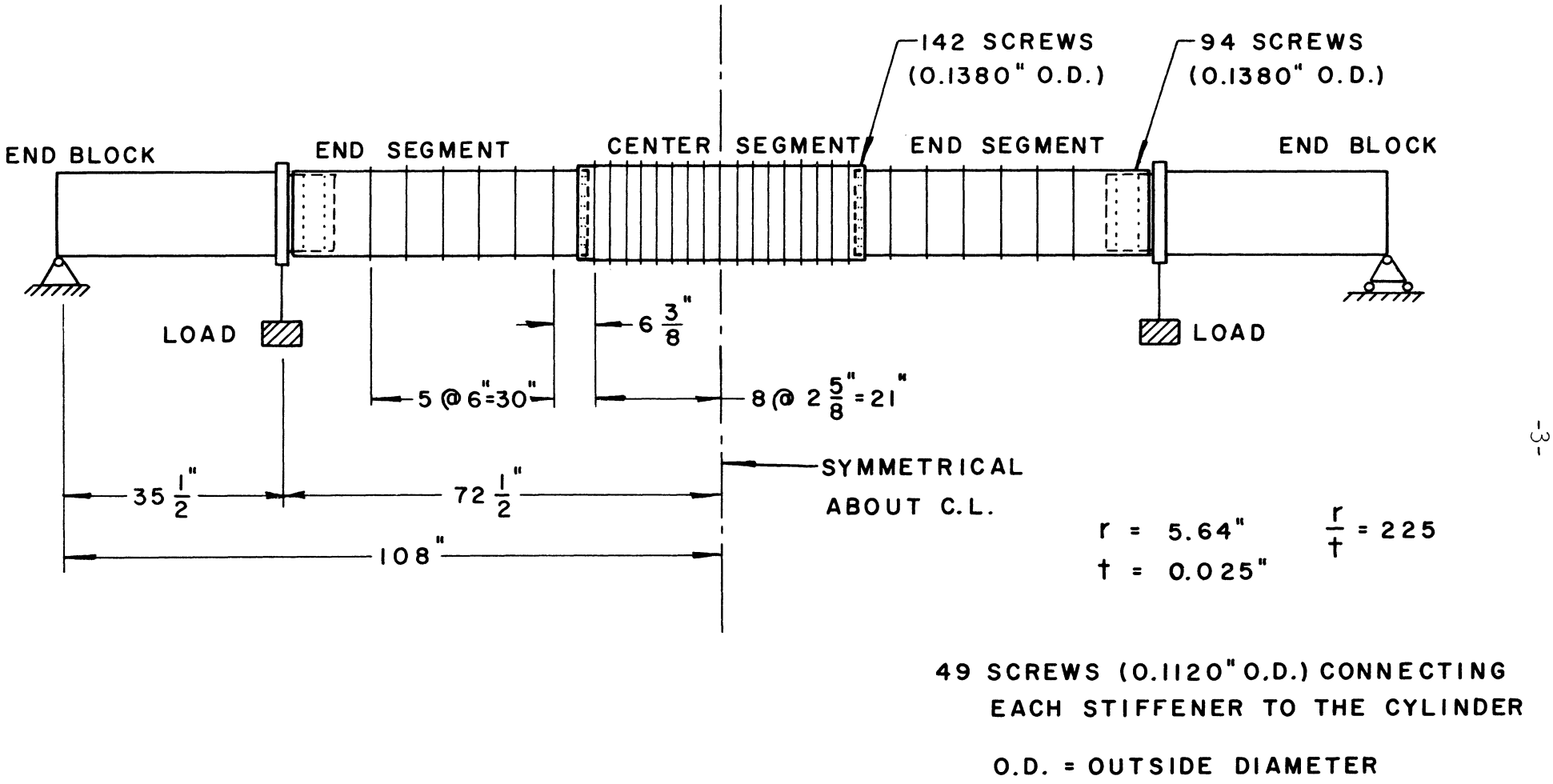

Figure 1. General Arrangement of the Model.

All the connections in the model were made by steel machine screws and nuts. The screws used in the splicing of the shell were 0.138" in outside diameter and those used to connect the stiffeners to the shell were 0.112" in outside diameter.

Two wooden end blocks were connected to the model for the purpose of end supports and application of the load.

As stated previously, the purpose of the test was to measure the stress variations on the stiffener. Nevertheless, a few AR-1 rectangular rosette gages were mounted on both the inside and outside of the shell for the purpose of detecting any unusual strains on the shell during the test.

Nine A-7 gages were placed on the stiffener located at the center of the model. Also A-7 gages were mounted on the inside of the shell opposite to those on the stiffener. All these electrical strain gages were Type SR4 manufactured by the Baldwin Lima-Hamilton Corporation.

A constant bending moment in the shell was obtained by loading both baskets simultaneously with equal increments of the load (Figure 1). One type of local loading was investigated, namely a uniformly distributed radial force applied at the top half of the cylinder. This was achieved by using loading baskets at the 14 locations shown in Tables II and III in which the load from the weights in the basket was assumed to be transmitted as a uniformly distributed radial force acting on the top half of the model.

Typical experimental results are given in Tables I and II for the 1/4" x 1/8" stiffener. The stresses due to the separate effect of

TABLE I

STRESSES ON THE OUTSIDE FACE OF THE STIFFENER, PSI
(Pure Bending)
+ Designates Tension

Spacing →	S = 2-5/8"					S = 5-1/4"				
Gage	Moments in-lbs.					Moments in-lbs.				
	3218	6744	11522	16299	21077	3218	6744	11522	16299	21077
1	+150	+275	+410	+ 475	+ 490	+150	+280	+397	+ 450	+ 435
2	+110	+205	+305	+ 363	+ 390	+ 85	+150	+210	+ 218	+ 163
3	+ 88	+180	+310	+ 440	+ 570	+ 55	+120	+230	+ 350	+ 485
4	+ 35	+105	+220	+ 355	+ 505	+ 20	+ 65	+190	+ 380	+ 615
5	+ 10	+ 35	+110	+ 235	+ 395	+ 15	+ 65	+185	+ 375	+ 620
6	- 15	- 18	- 5	+ 35	+ 95	+ 3	+ 25	+ 75	+ 165	+ 300
7	- 95	-190	-325	- 465	- 600	- 45	-105	-205	- 330	- 465
8	-105	-230	-430	- 655	- 945	-110	-250	-480	- 760	-1080
9	-155	-345	-665	-1025	-1435	-180	-400	-770	-1160	-1615

Spacing →	S = 10-1/2"					S = 21"				
Gage	Moments in-lbs.					Moments in-lbs.				
	3218	6744	11522	16299	21077	3218	6744	11522	16299	21077
1	+135	+250	+345	+ 325	+ 215	+140	+250	+300	+ 300	+ 200
2	+ 80	+130	+150	+ 115	+ 5	- 10	- 20	- 50	- 210	- 780
3	+ 65	+130	+220	+ 315	+ 400	+ 40	+ 90	+160	+ 260	+ 200
4	+ 50	+135	+305	+ 555	+ 840	+ 40	+110	+270	+ 580	+1180
5	+ 35	+ 90	+240	+ 475	+ 765	+ 40	+120	+260	+ 540	+1020
6	- 8	0	+ 45	+ 135	+ 310	+ 20	+ 40	+100	+ 190	+ 350
7	- 55	-120	-215	- 320	- 460	- 80	-130	-210	- 300	- 540
8	-120	-270	-515	- 820	-1170	- 70	-200	-440	- 720	-1150
9	-200	-435	-820	-1285	-1805	-180	-400	-780	-1240	-1820

$\frac{1}{4}$" x $\frac{1}{8}$"

Stiffeners

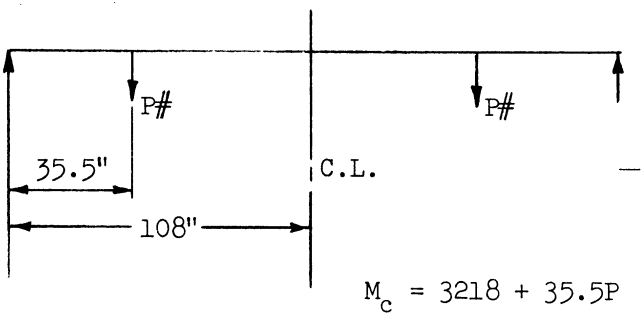

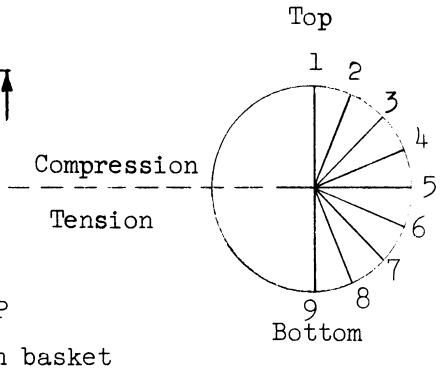

$M_c = 3218 + 35.5P$

where P = Load on each basket

Loading Condition

TABLE II

STRESSES ON THE OUTSIDE FACE OF THE STIFFENER, PSI
(Local Loading)
+ Designates Tension

Spacing →	S = 2-5/8"					S = 5-1/4"				
Gage	Moments in-lbs.					Moments in-lbs.				
	3218	6744	11522	16299	21077	3218	6744	11522	16299	21077
1	+150	+510	+ 990	+1460	+1880	+150	+730	+1490	+2210	+2850
2	+110	+320	+ 590	+ 820	+1020	+ 85	+345	+ 685	+1015	+1255
3	+ 88	+ 63	- 7	- 127	- 267	+ 55	-165	- 475	- 785	-1105
4	+ 35	-165	- 445	- 745	-1035	+ 20	-460	-1110	-1750	-2340
5	+ 10	+ 30	+ 100	+ 200	+ 340	+ 15	+ 45	+ 165	+ 315	+ 525
6	- 15	+315	+ 765	+1225	+1715	+ 3	+623	+1503	+2413	+3323
7	- 95	- 15	+ 105	+ 205	+ 295	- 45	+165	+ 455	+ 715	+ 965
8	-105	-325	- 645	-1025	-1425	-110	-420	- 940	-1500	-2080
9	-155	-575	-1185	-1855	-2545	-180	-800	-1710	-2690	-3680

Spacing →	S = 10-1/2"					S = 21"				
Gage	Moment in-lbs.					Moment in-lbs.				
	3218	6744	11522	16299	21077	3218	6744	11522	16299	21077
1	+135	+995	+2115	+3165	+4135	+140	+1460	+3000	+4540	+6010
2	+ 80	+460	+ 960	+1400	+1810	- 10	+ 640	+1260	+1850	+2310
3	+ 65	-355	- 915	-1525	-2105	+ 40	- 600	-1560	-2500	-3470
4	+ 50	-780	-1910	-3030	-4080	+ 40	-1540	-3360	-5080	-6710
5	+ 35	+ 95	+ 265	+ 475	+ 725	+ 40	+ 290	+ 460	+ 720	+1080
6	- 8	+1032	+2442	+3932	+5382	+ 20	+1680	+3750	+5850	+7990
7	- 55	+ 255	+ 745	+1195	+1615	- 80	+ 520	+1210	+1860	+2450
8	-120	- 590	-1290	-2030	-2820	- 70	- 720	-1680	-2720	-3780
9	-200	-1120	-2380	-3680	-5010	-180	-1380	-3040	-4730	-6430

$\frac{1}{4}$" x $\frac{1}{8}$" Stiffeners

W lbs.	M_c in.-lbs.
0	3218
5-1/6	6744
12-1/6	11522
19-1/6	16299
26-1/6	21077

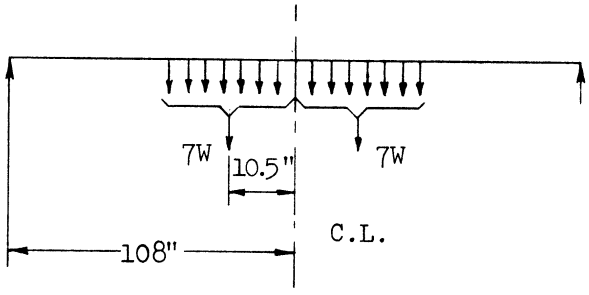

$M_c = 3218 + 682.5W$

where W = Load on each basket in lbs.

Loading Condition

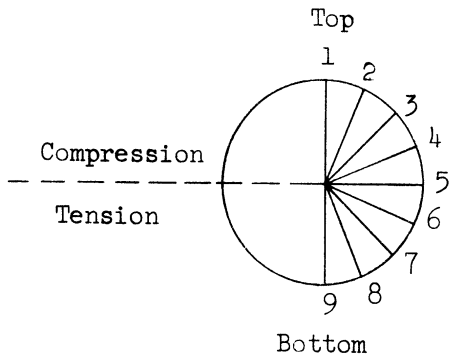

the local loading which are given in Table III are obtained by subtracting the stresses of Table I from those of Table II. The moment of 3218 in-lbs. which appears in the tables is the moment at the center of the model due to the weight of the cylinder, the end blocks and the end loading baskets.

The strains in the gages on the inside of the shell and opposite to those on the outside face of the stiffener are affected appreciably by any local longitudinal bending and other local conditions, which are difficult to evaluate. For this reason these strains were ignored because it was felt that they could not be used to advantage in the evaluation of the data.

The variation in the stress on the outside face of the 1/4" x 1/8" stiffener as a function of the applied pure bending moment on the cylinder, is given graphically in Figure 2. These stresses are plotted for five locations on the stiffener and for a stiffener spacing of 10-1/2 inches.

The nine strain locations on the stiffener start with No. 1 at the top of the stiffener (compressive side of the cylinder) and are spaced at 22.5 degrees around the stiffener with No. 9 located at the bottom of the stiffener (tension half of the cylinder). These locations are shown in Tables I, II, and III.

INTERPRETATION OF THE DATA

A study of the curves in Figure 2 shows that the variation of the stress at any point in the stiffener is a nonlinear function of the applied pure bending moment on the cylinder, especially at Points 1, 5 and 9 (top, center and bottom of the stiffener). One also observes that the tensile stress on the outside face of the stiffener at Point 1,

TABLE III

STRESSES ON THE OUTSIDE FACE OF THE STIFFENER
DUE TO THE SEPARATE EFFECT OF THE LOCAL LOADING, PSI
(Local Loading Minus Bending)
+ Designates Tension

Spacing →	S = 2-5/8"				S = 5-1/4"			
Gage	Load W lbs.				Load W lbs.			
	5-1/6	12-1/6	19-1/6	26-1/6	5-1/6	12-1/6	19-1/6	26-1/6
1	+ 235	+ 580	+ 985	+1390	+ 450	+1093	+1760	+2415
2	+ 115	+ 285	+ 457	+ 630	+ 195	+ 475	+ 797	+1092
3	- 117	- 317	- 567	- 837	- 285	- 705	-1135	-1590
4	- 270	- 665	-1100	-1540	- 525	-1300	-2130	-2955
5	- 5	- 10	- 35	- 55	- 20	- 20	- 60	- 95
6	+ 333	+ 770	+1190	+1620	+ 598	+1428	+2248	+3023
7	+ 175	+ 430	+ 670	+ 895	+ 270	+ 660	+1045	+1430
8	- 95	- 215	- 370	- 480	- 170	- 460	- 740	-1000
9	- 230	- 520	-830	-1110	- 400	- 940	-1530	-2065

Spacing →	S = 10-1/2"				S = 21"			
Gage	Load W lbs.				Load W lbs.			
	5-1/6	12-1/6	19-1/6	26-1/6	5-1/6	12-1/6	19-1/6	26-1/6
1	+ 745	+1770	+2840	+3920	+1210	+2700	+4240	+5810
2	+ 330	+ 810	+1285	+1805	+ 660	+1310	+2060	+3090
3	- 485	-1135	-1840	-2505	- 690	-1720	-2760	-3670
4	- 915	-2215	-3585	-4920	-1650	-3630	-5660	-5530
5	+ 5	+ 25	0	- 40	+ 170	+ 200	+ 180	+ 60
6	+1032	+2397	+3797	+5072	+1640	+3650	+5660	+7640
7	+ 375	+ 960	+1515	+2075	+ 650	+1420	+2160	+2990
8	- 320	- 775	-1210	-1650	- 520	-1240	-2000	-2630
9	- 685	-1560	-2395	-3205	- 980	-2260	-3490	-4610

1" x 1"
4 8

Stiffeners

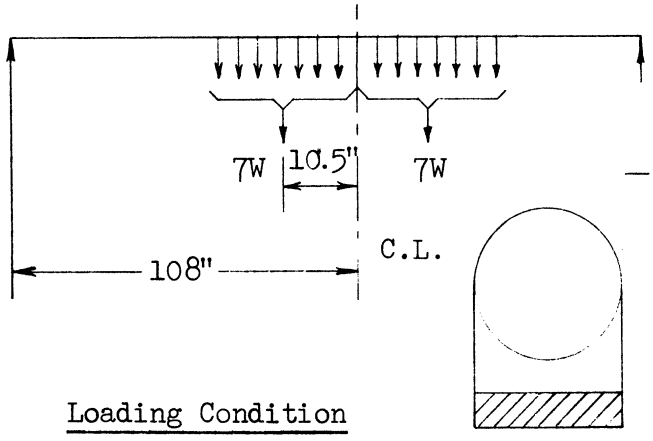

Loading Condition

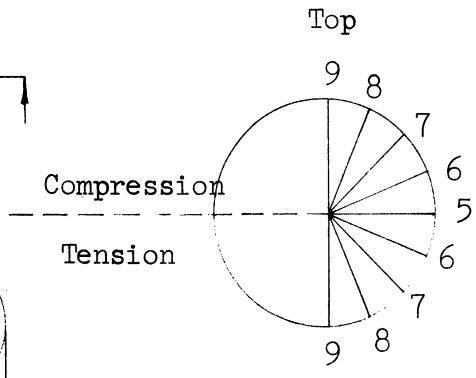

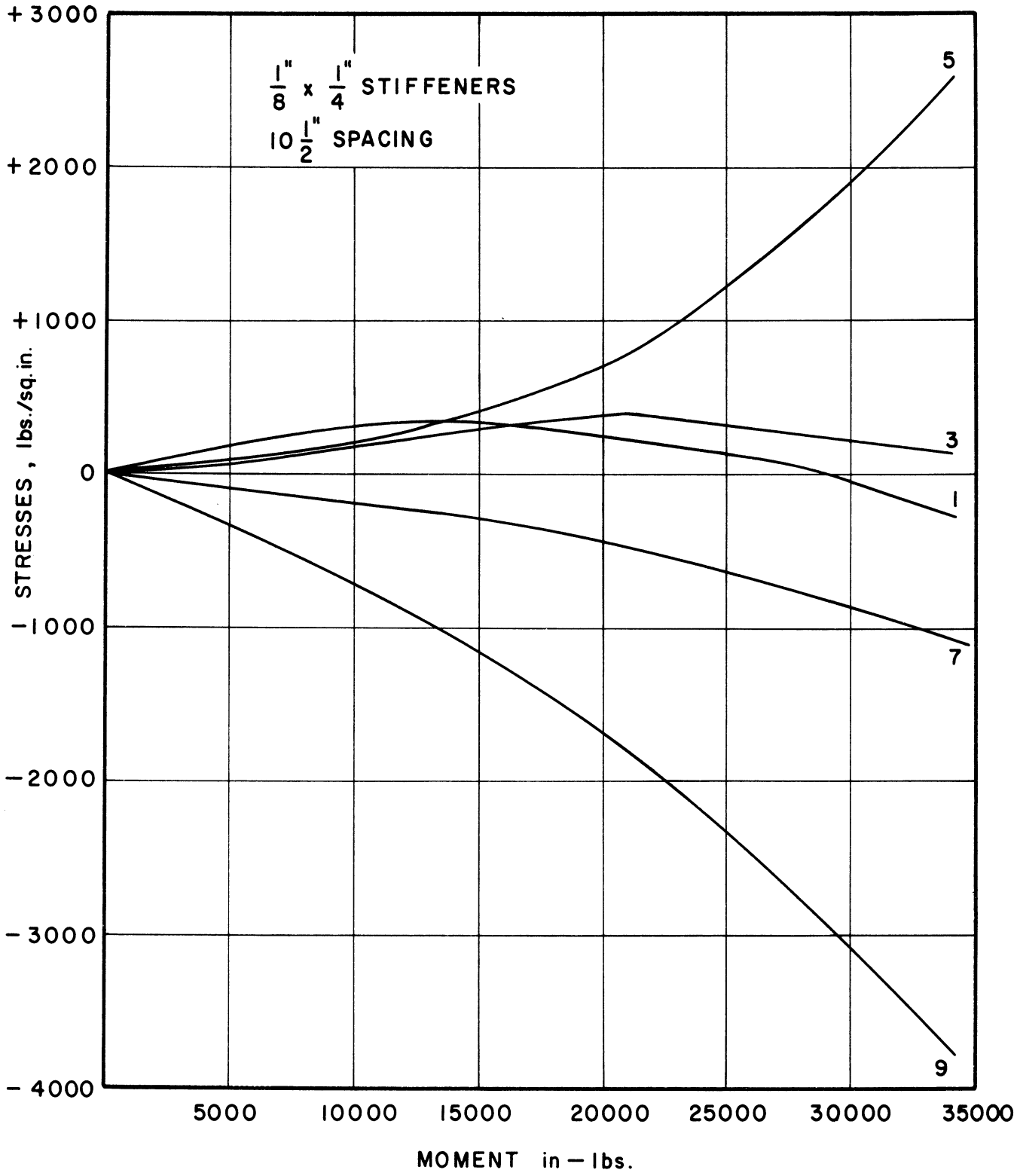

Figure 2. Stresses on the Outside Face of the Stiffener vs. Pure Applied Bending Moment.

increases nonlinearly until the applied bending moment reaches a certain value, after which the tensile stress begins to decrease with the increase of the moment. On the other hand, the stress at Point 9 increases with the increase of the applied moment and with no reversal in the increments of the stress.

The above behavior suggests that the stresses on the stiffener, due to an applied pure bending moment on the cylinder, are caused by more than one type of action. Two types of action can be given to explain the above stress behavior. They are: (1) the flattening of the cylinder, i.e., an increase in the horizontal diameter and a decrease in the vertical diameter of the cylinder. This is caused by the curvature of the cylinder when subjected to bending, whereby the longitudinal stresses at both the top and bottom halves of the cylinder will have resultant forces acting towards the center of the cylinder, thus causing it to flatten. (See Figure 4); (2) the increase of the radii of the cylinder on the compression side and their decrease on the tension side due to Poisson's ratio. This action will be referred to as the bulging of the cylinder.

Figure 3 shows the types of stresses on the outside face of the stiffener due to the two types of action, the flattening and the bulging. Both of these two actions have the same sign of stress at Point 9 and opposite signs at Point 1. At Point 5 flattening will be the main contributing factor to the stress, while bulging will be the main contributing factor to the stress at Points 3 and 7.

A study of Figure 3 explains the behavior of the stresses in Figure 2 and points to the fact that the stresses due to flattening vary at a faster rate than their variation due to bulging.

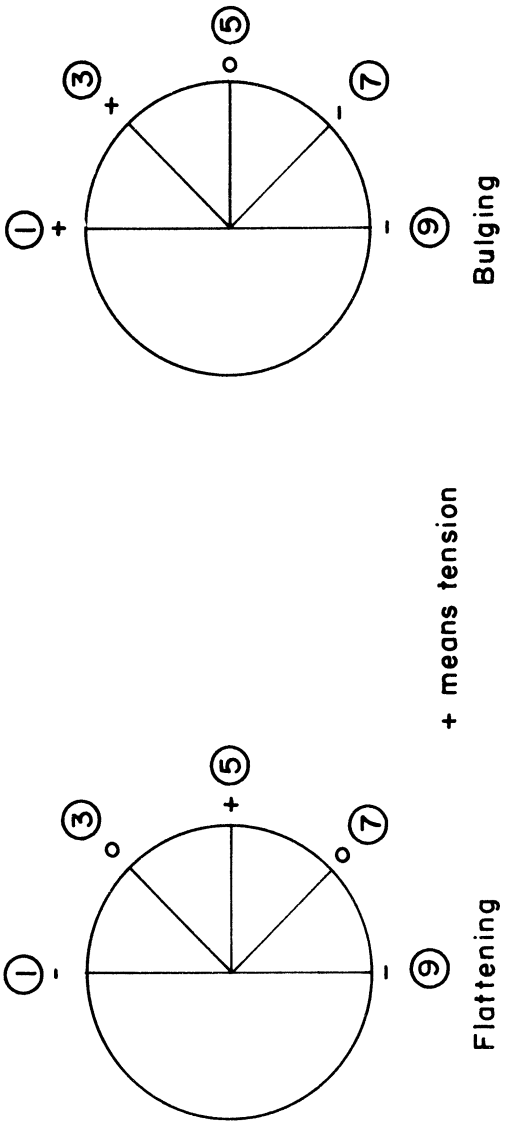

Figure 3. Types of Stress on the Outside Face of the Stiffener.

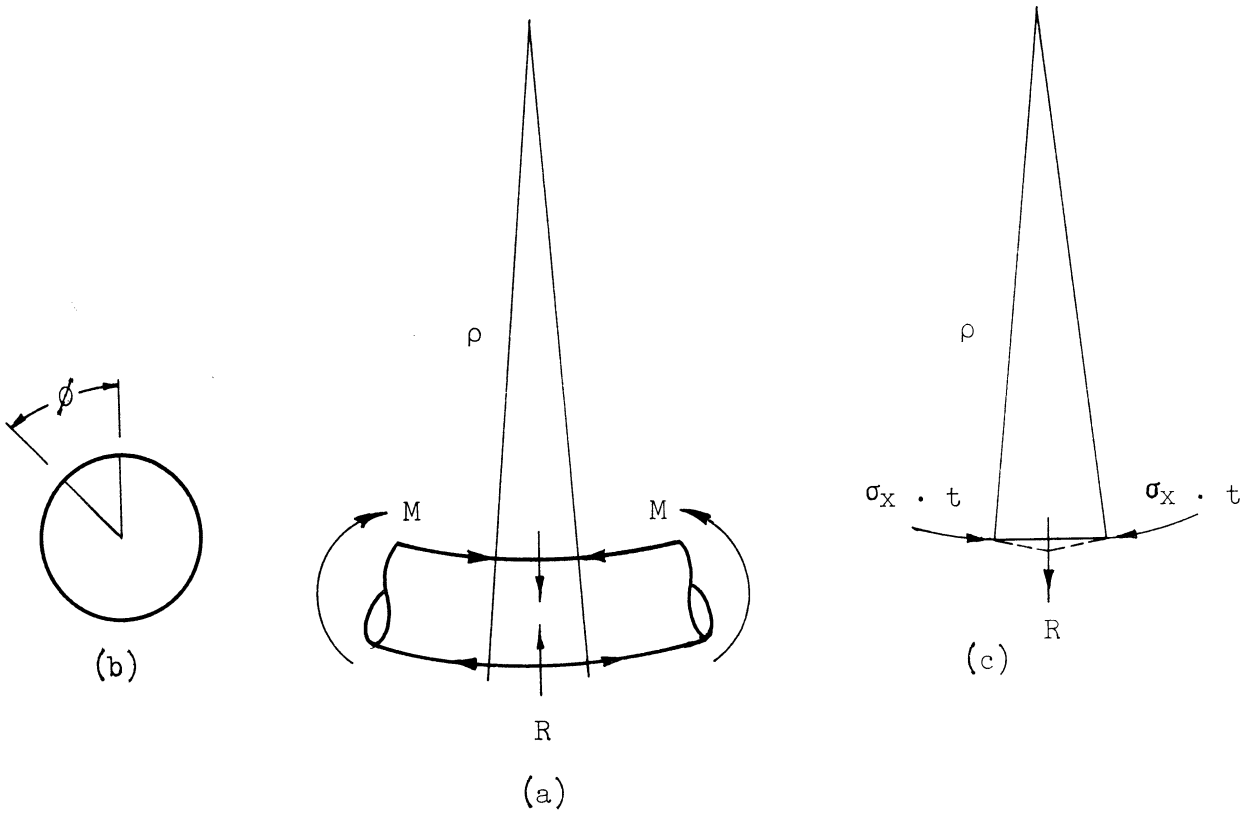

Figure 4. Illustration of the Flattening of the Cylinder.

THEORETICAL INVESTIGATION AND CORRELATION WITH THE EXPERIMENTAL RESULTS

The Effect of the Flattening of the Cylinder

The flattening of the cylinder is illustrated in Figure 4, where both the compressive and tensile longitudinal stresses at the top and bottom halves of the cylinder respectively, have resultant forces, R, parallel to the plane of bending (vertical forces) and acting toward the inside of the cylinder. The longitudinal stress σ_x at any angle ϕ measured from the vertical as shown in Figure 4b is equal to:

$$\sigma_x = -\frac{Er}{\rho} \cos \phi \qquad (1)$$

The resultant of the longitudinal stresses acting toward the inside of the cylinder can be computed at any angle ϕ by considering a unit length both transversely and longitudinally. The value of R per unit of surface (see Figure 4c) will be equal to:

$$R = \frac{Ert}{\rho^2} \cos \phi \qquad (2)$$

The flattening of the cylinder is therefore equivalent to subjecting it to vertical pressure whose magnitude is $\frac{Ert}{\rho^2} \cos \phi$ per unit circumferential area as was noted by Brazier.[1] The distribution of the forces on any stiffener, due to the flattening of the cylinder, are assumed to vary according to the variation of the pressure on the cylinder as shown in Figure 5. It should be mentioned that a vertical force of p cos ϕ /circumferential unit length is equal to p/horizontal unit length.

The bending moments and the normal forces in the stiffener subjected to the flattening forces of Figure 5, are given by the following

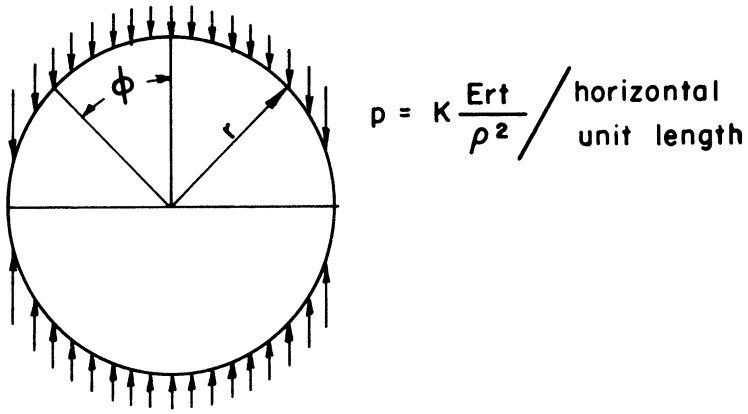

Figure 5. Distribution of the Forces Acting on a Ring Stiffener Due to the Flattening of the Cylinder.

equations:

$$M_r = - K \frac{Er^3t}{4\rho^2} \cos 2\phi \tag{3}$$

$$N_r = - K \frac{Er^2t}{\rho^2} \sin^2 \phi \tag{4}$$

where K, which has the unit of length is a function of a complex nature varying with the spacing "S" of the stiffeners and with the other parameters of the problem.

Equation (3) shows that the moments in the stiffener vary proportionally to the square of the curvature of the cylinder $1/\rho$. The curvature of a long unstiffened cylinder subjected to pure bending varies nonlinearly with the moment, due to the progressive flattening of the cylinder as was pointed out by Brazier.[1] The relationship between the moment and the curvature as was derived by Brazier is given by the following equation

$$M = \frac{E\pi r^3t}{2} \left[\frac{2}{\rho} - \frac{3r^4(1-\mu^2)}{\rho^3t^2}\right] \tag{5}$$

If no progressive flattening is assumed then the moment is related to the curvature by:

$$M = \frac{E\pi r^3t}{\rho} \tag{6}$$

Both equations above are plotted in Figure 6 for the model considered in this paper.

For a stiffened cylinder the true curve, expressing the relationship between the applied bending moment and the curvature, although not quantitatively determinable, should fall between Curves 1 and 2 (Figure 6).

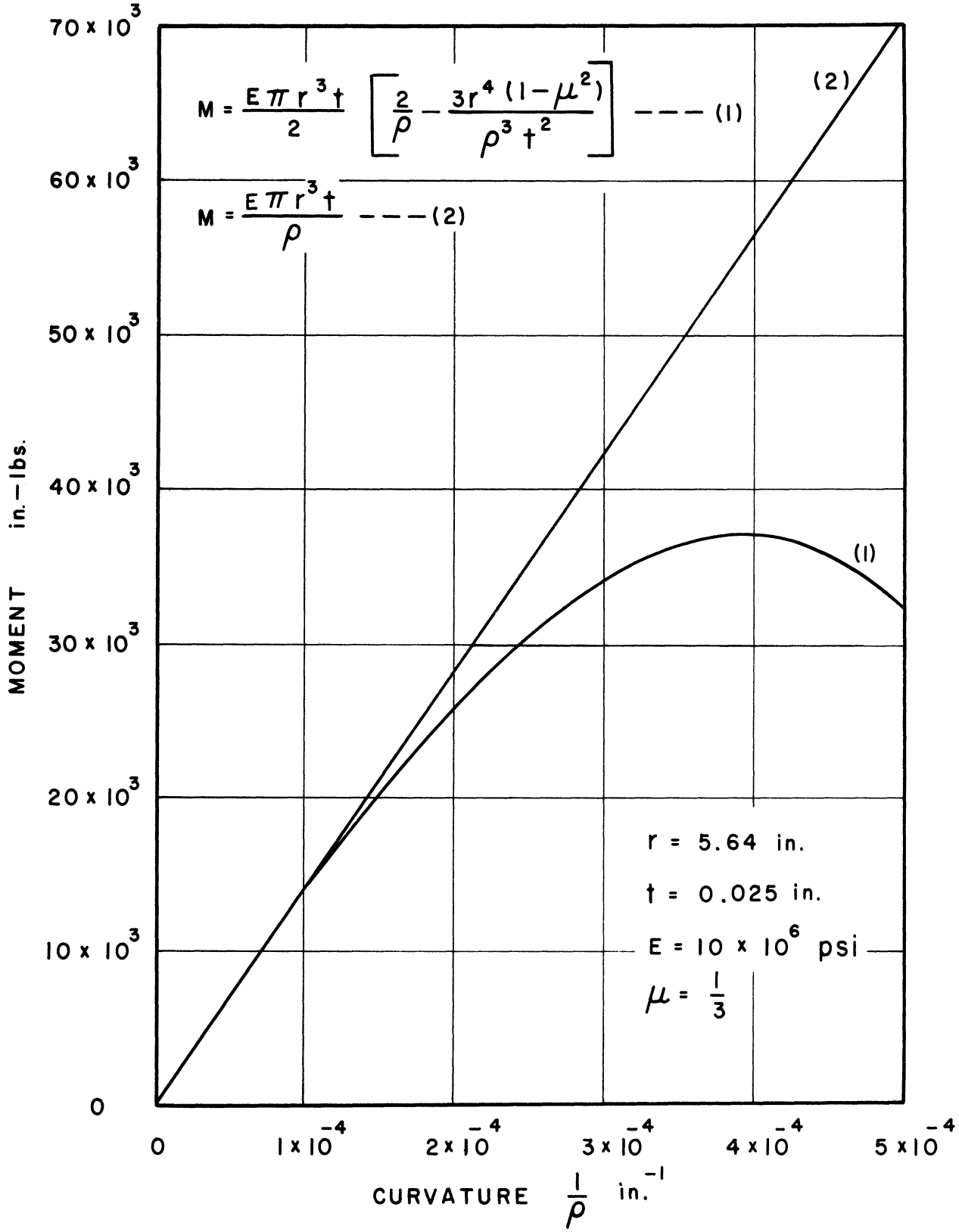

Figure 6. Moment vs. Curvature - Long Unstiffened Cylinder (Model).

It is reasonable to assume, however, that the curvature, $1/\rho$, varies linearly with the moment as given by Curve 2 especially for the lower values of M where the divergence between the two curves is negligible. On the other hand the use of an assumed curve falling between (1) and (2) is more justifiable for the higher values of the applied pure bending moment.

Figure 7 shows a comparative plotting of the stresses on the outside face of the stiffener at Point 5, due to flattening, as a function of the applied bending moment on the cylinder. The experimental stresses at Point 5 from the pure bending moment tests on the cylinder are assumed to be caused only by flattening. Both the experimental and theoretical stresses are plotted relative to the stress when M = 11522 in-lbs. This stress when M = 11522 in-lbs. is taken to be equal to unity. The good agreement between the theoretical curves and the experimental results justifies the assumed forces of Figure 5.

For closely spaced rings, the flattening forces can be assumed to be entirely resisted by the stiffeners in which case K can be taken equal to S. The bending moments in the stiffener will therefore reduce to:

$$M_r = - S \frac{Er^3t}{4 \rho^2} \cos 2\phi \qquad (7)$$

If ρ, which is the radius of curvature of the cylinder, is taken equal to EI/M, then the moments in the stiffener, M_r, will take the form:

$$M_r = - \frac{1}{4\pi^2 r^3 t} \frac{M^2}{E} S \cos 2\phi \qquad (8)$$

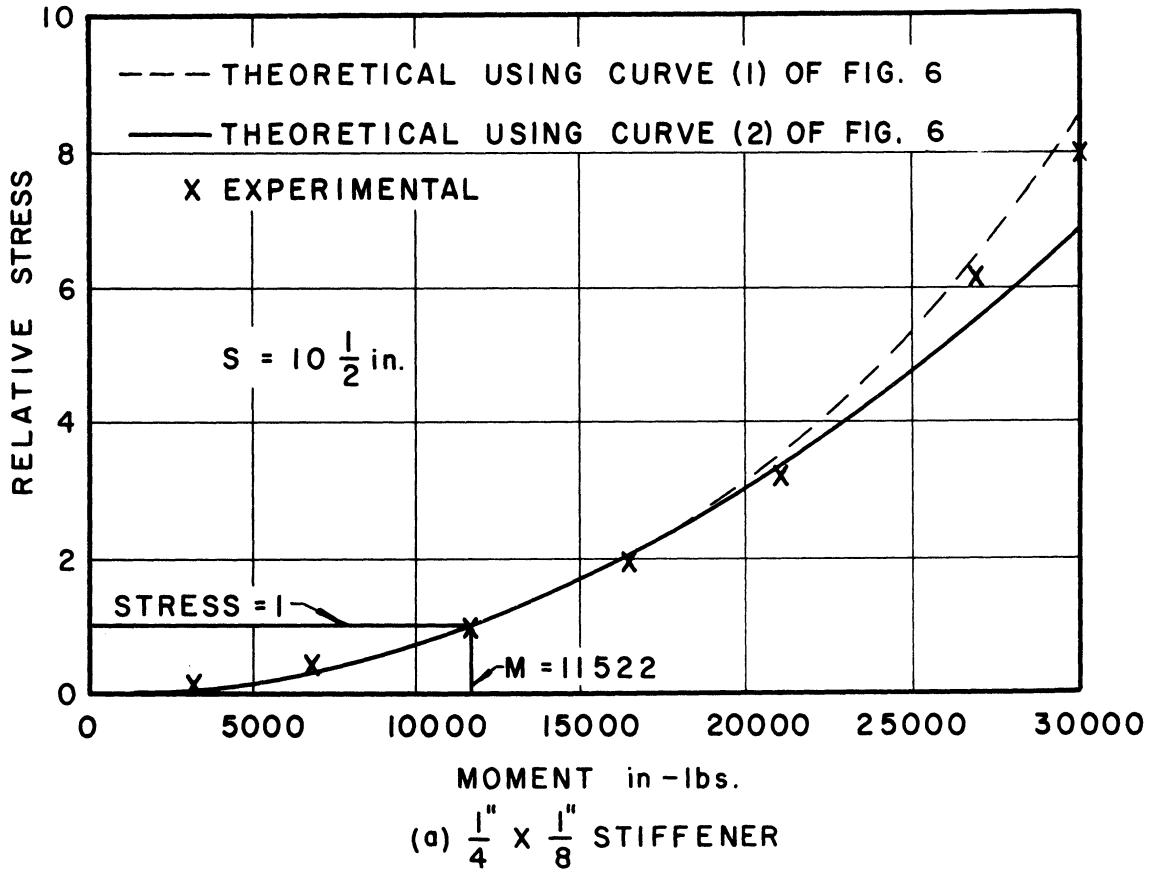

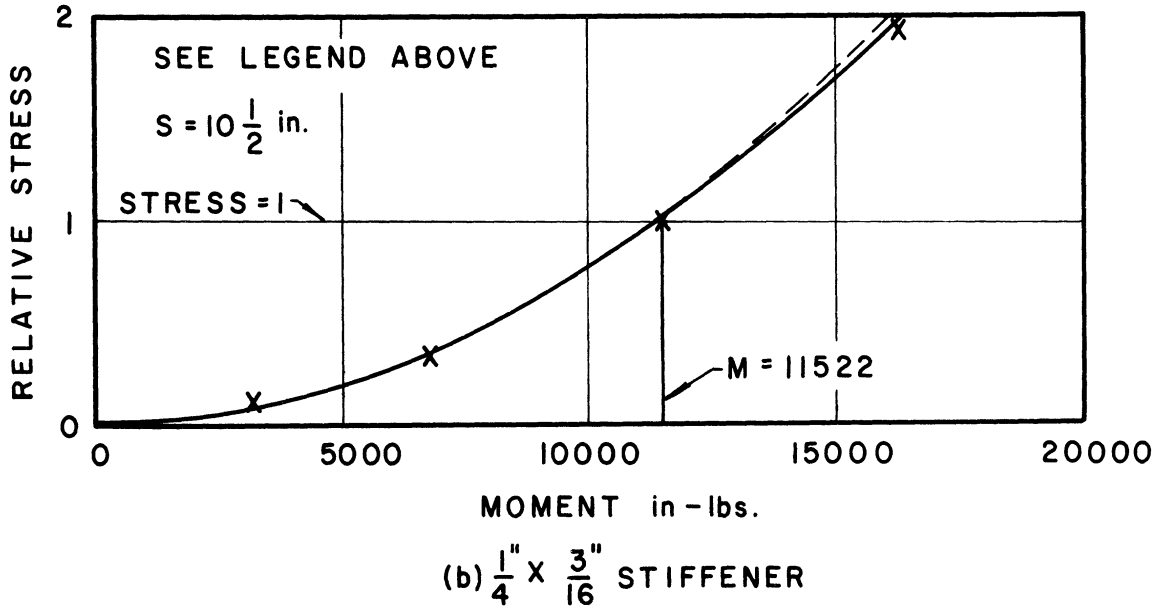

Figure 7. Relative Stress vs. Moment (Flattening).

where

I is the moment of inertia of the cylinder, taken equal to $\pi r^3 t$

M is the applied pure bending moment on the cylinder.

Equation (8) gives an approximate formula for determining the bending moments in a ring stiffener due to flattening. A better approximation, however, can be obtained by establishing a more accurate value for the function K. The following paragraphs present the procedure used to establish the major parameters of K.

The vertical pressure acting on the cylinder as a result of its flattening will be resisted in both the transverse and longitudinal directions. This resistance can be closely approximated by assuming that it is similar to a beam subjected to a uniform transverse load and supported on an elastic foundation. The parameters of K can therefore be obtained by studying the analogous problem of an infinitely long beam (Figure 8) loaded by a uniformly distributed load q, and uniformly supported by an elastic support whose spring constant is K_1. The continuous beam is also supported at different points by concentrated elastic supports whose spacing is equal to "S" and whose spring constant is K_2.

The magnitude of the force F in any one of the concentrated elastic supports can be obtained by the method of superposition as illustrated in Figure 9. Figure 9a shows the elastically supported beam acted on by the uniformly distributed load q and Figure 9b shows the elastically supported beam acted on by the concentrated loads (F forces). The deflection Δ_1 of Figure 9a is simply equal to: $\Delta_1 = q/K_1$.

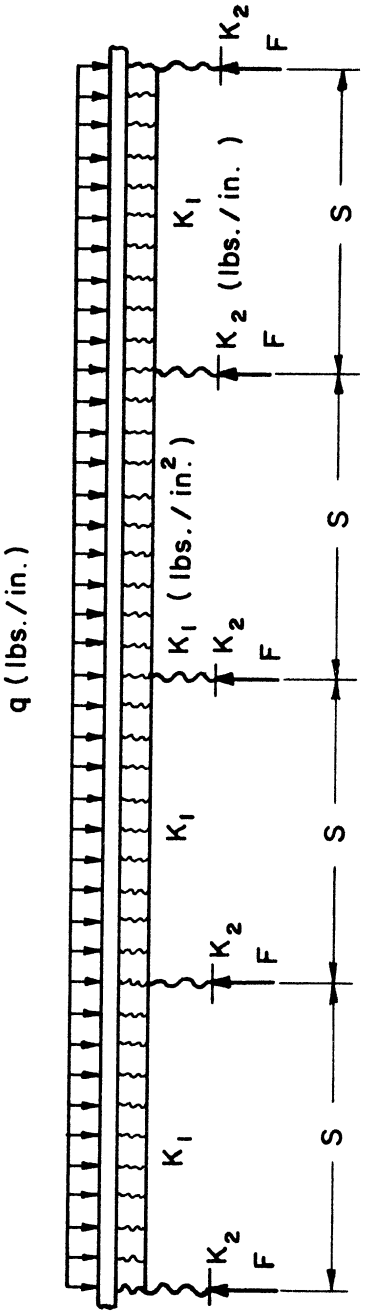

Figure 8. Infinitely Long Beam on Elastic Supports.

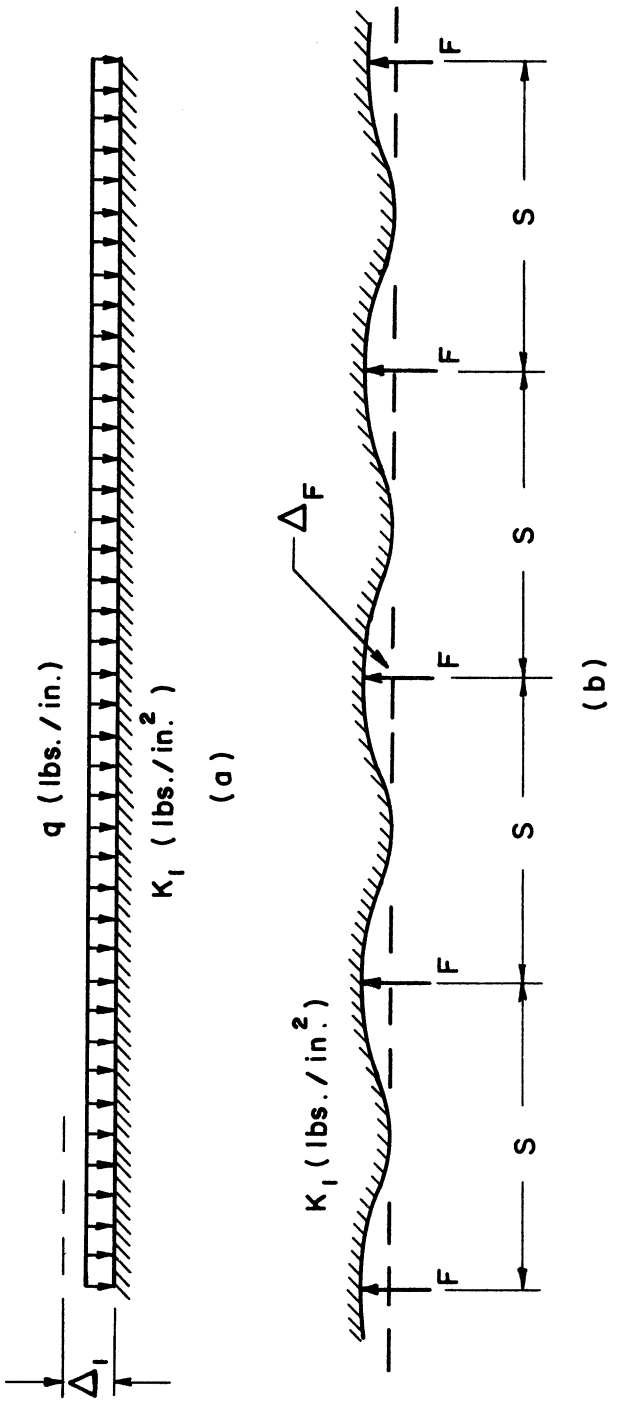

Figure 9. Infinitely Long Beam on Elastic Supports.

The deflection Δ_F (Figure 9b) due to the system of concentrated supports should be equal to Δ_1 minus the deformation in the elastic concentrated support. This relationship can be written in the following form:

$$\Delta_F = \frac{q}{K_1} - \frac{F}{K_2} \tag{9}$$

The value of Δ_F can be obtained by the use of the reciprocal theorem making use of the displacement curve of an elastically supported, infinitely long beam, acted on by a unit concentrated load as shown in Figure 10. The displacement curve[4] is given by the following equation:

$$y = \frac{\lambda}{2K_1} [e^{-\lambda x} (\cos \lambda x + \sin \lambda x)] \tag{10}$$

where

$$\lambda = \sqrt[4]{\frac{K_1}{4EI}}$$

E = the modulus of Elasticity of the beam

I = the moment of Inertia of the beam.

Using the reciprocal theorem, the deflection Δ_F of Figure 9b will be therefore equal to

$$\Delta_F = F \frac{\lambda}{2K_1} [1 + 2 \sum_{n=1}^{\infty} e^{-n\lambda s} (\cos n\lambda s + \sin n\lambda s] \tag{11}$$

If the value of Δ_F as given above is substituted in Equation (9), then F can be written in the following form:

$$F = \frac{q}{\frac{\lambda}{2} [1 + 2 \sum_{n=1}^{\infty} e^{-n\lambda s} (\cos n\lambda s + \sin n\lambda s)] + \frac{K_1}{K_2}} \tag{12}$$

---

[4] See for example page 11 of: Hetenyi, M. Beams on Elastic Foundation. The University of Michigan Press, Ann Arbor, Michigan, 1946.

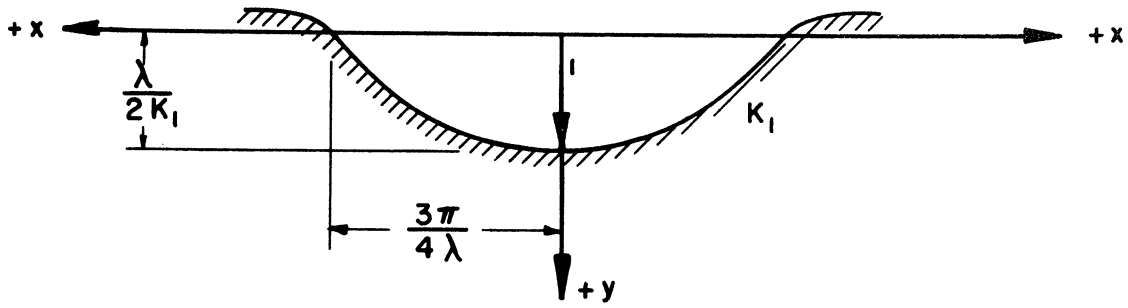

Figure 10. Infinitely Long Beam on an Elastic Support Loaded by a Unit Concentrated Load.

If we let

$$[1 + 2 \sum_{n=1}^{\infty} e^{-nx} (\cos nx + \sin nx)] = \psi(x) \qquad (13)$$

Then the force F of Equation (12) will be written in the form:

$$F = \frac{q}{\frac{\lambda}{2} [\psi(\lambda s)] + \frac{K_1}{K_2}} \qquad (14)$$

The resistance of the stiffeners when subjected to the flattening action will be analogous to the resistance of the concentrated elastic supports, while the resistance of the shell will be analogous to the resistance of the uniformly distributed elastic supports. Therefore the forces on the stiffeners $K \frac{Ert}{\rho^2}$ (Figure 5) will be assumed to have the same form as the force F of Equation (14), in which case $\frac{Ert}{\rho^2}$ will be equivalent to q and K will be equivalent to $\frac{1}{\frac{\lambda}{2} [\psi(\lambda s)] + \frac{K_1}{K_2}}$. The parameters of K can therefore be obtained in the following manner:

$$K_1 \sim \frac{Et^3}{r^4} \qquad K_2 \sim \frac{EI_r}{r^4} \qquad I \sim t^3$$

$$\therefore \quad \frac{K_1}{K_2} \sim \frac{t^3}{I_r} \quad \text{or} \quad \frac{K_1}{K_2} = C_1 \frac{t^3}{I_r}$$

$$\lambda \sim \sqrt[4]{\frac{1}{r^4}} \quad \text{or} \quad \lambda = \frac{C_2}{r}$$

where

t = thickness of the cylinder

r = mean radius of the cylinder (assumed equal to mean radius of the rings)

I_r = moment of inertia of the ring stiffener

C_1 = constant

C_2 = constant

The function K will therefore take the form

$$K = \frac{1}{\frac{\lambda}{2}\left[\psi(\lambda s)\right] + C_1 \frac{t^3}{I_r}} \qquad (15)$$

where

$$\lambda = \frac{C_2}{r} .$$

The experimental results are used to establish average values for the constants C_1 and C_2. The experimental stresses due to flattening were separated from the pure bending moment tests by assuming that the stresses at Point 5 are caused only by flattening and that the variation of the stresses around the stiffener due to flattening are proportional to cos 2ϕ. Both the results obtained from the 1/4" x 1/8" and the 1/4" x 3/16" stiffeners were used to determine values of C_1 and C_2 that will best fit all the available experimental results. The effective width of the shell acting as an integral part of the stiffener was taken to be equal to 24 times the thickness of the shell.

The determined values of C_1 and C_2 are:

$C_1 = 1.0$

$C_2 = 1.1$

Figure 11 gives the variation of both calculated and experimental stress in the stiffener, due to flattening, at Points 1 and 9 (top and bottom of the stiffener) as a function of the spacing of the stiffeners.

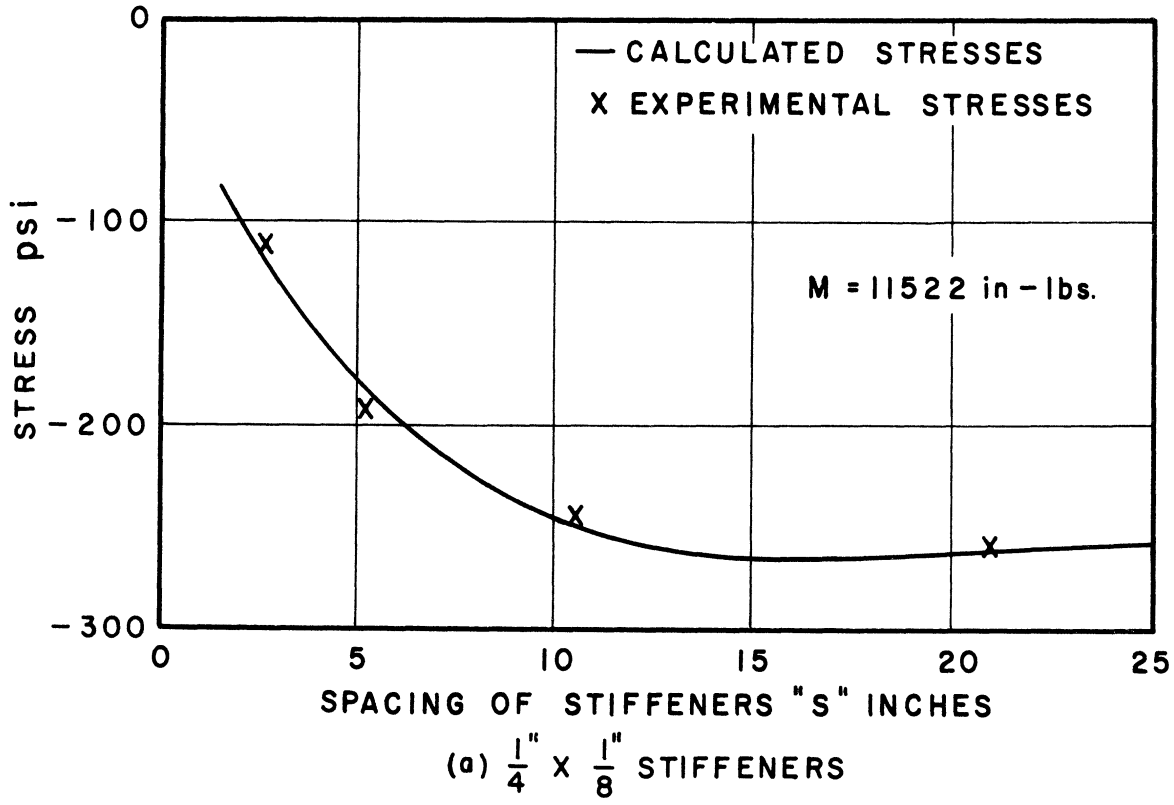

(a) $\frac{1}{4}$" X $\frac{1}{8}$" STIFFENERS

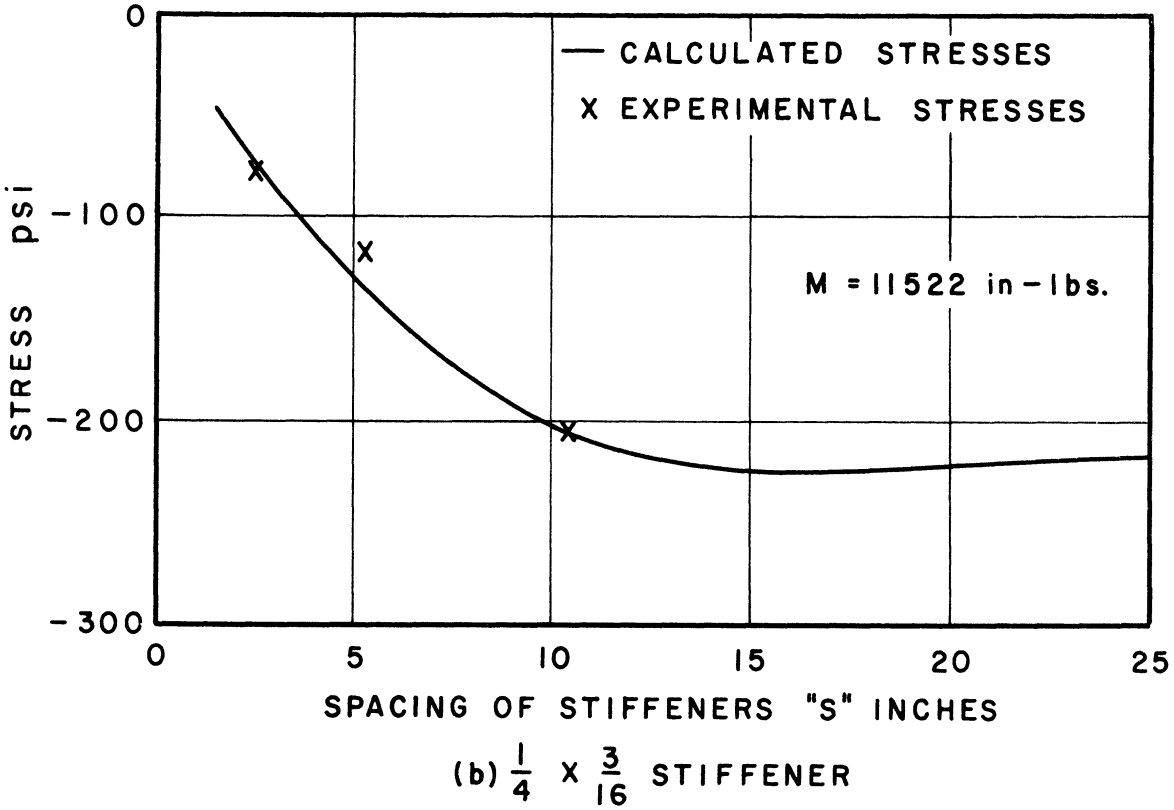

(b) $\frac{1}{4}$ X $\frac{3}{16}$ STIFFENER

Figure 11. Stresses on the Outside Face of the Stiffener at Top or Bottom vs. the Spacing of the Stiffeners (Flattening).

The calculated stresses were obtained by using Equations (3), (4), and (15). The good agreement between the calculated and experimental stresses justifies the general form of Equation (15).

The Effect of the Bulging of the Cylinder

The bulging of the cylinder is caused by the increase of the radii in the compression half and a decrease in the tension half of the cylinder due to Poisson's ratio. The longitudinal stresses in the cylinder due to an applied pure bending moment will be equal to:

$$\sigma_x = - \frac{M}{\pi r^2 t} \cos \phi \qquad (16)$$

where ϕ is measured as shown in Figure 12. The distortion of the cross-section from its originally circular shape can be written in the form:

$$\delta = \frac{\mu M}{\pi r t E} \cos \phi \qquad (17)$$

The distribution of the radial forces on the stiffeners will be assumed to be proportional to the radial displacement δ or equal to $Z \cos \phi$. The tangential forces will be assumed to be $Z \sin \phi$ which will satisfy the equilibrium conditions (see Figure 13).

If the shear and normal deformations are ignored, then the loading of Figure 13 produces no bending moments in the ring, a condition which indicates that the total strain energy in the ring is approaching a minimum. For this condition of no bending moments, the normal forces in the ring will be given by the following equation:

$$N_r = Zr \cos \phi \qquad (18)$$

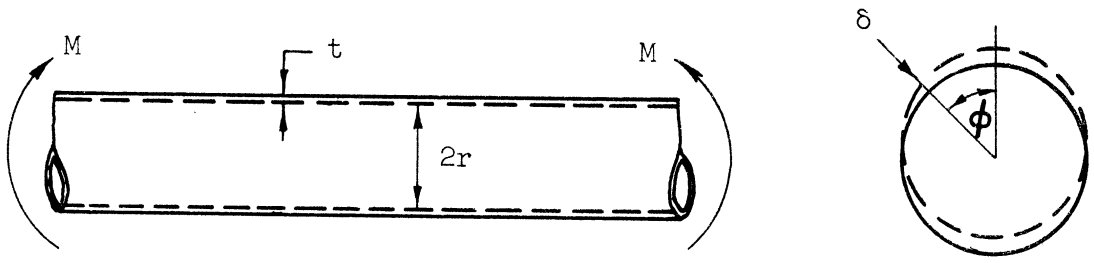

Figure 12. Illustration of the Bulging of the Cylinder.

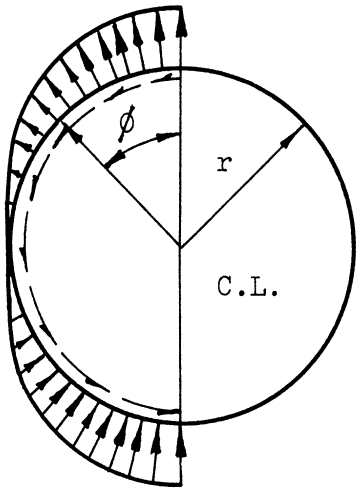

Radial Forces = Z cos ϕ
Tangential Forces = Z sin ϕ

Symmetrical about C.L.

Figure 13. Distribution of the Forces Acting on a Ring Stiffener Due to the Bulging of the Cylinder.

The stiffners due to bulging of the cylinder, are therefore mainly subjected to normal forces. For this reason the major parameters of Z of Figure 13 can be obtained by utilizing the solution of the following similar problem. Consider an infinitely long cylinder subjected to uniformly distributed line loads, acting along different circular sections and spaced at a distance "S" (Figure 14).

The radial displacement of the cylinder under any one of the "F" loads can be obtained by the reciprocal theorem if one uses the solution of an infinitely long cylinder loaded uniformly along one circular section as shown in Figure 15.

The radial displacements of the cylinder of Figure 15 are given by the equation:[5]

$$y = \frac{Fr^2\beta}{2Et} e^{-\beta x} (\sin \beta x + \cos \beta x) \qquad (19)$$

where

$$\beta^4 = \frac{3(1 - \mu^2)}{r^2t^2}$$

Using the reciprocal theorem the radial displacement, Δ_F, of Figure 14 can therefore be written in the form:

$$\Delta_F = \frac{Fr^2\beta}{2Et} [1 + 2 \sum_{n=1}^{\infty} e^{-n\beta s} (\sin n\beta s + \cos n\beta s)]$$

But

$$[1 + 2 \sum_{n=1}^{\infty} e^{-n\beta s} (\sin n\beta s + \cos n\beta s)] = \psi(\beta s)$$

---

[5] See page 396: Timoshenko, S. Theory of Plates and Shells, New York and London: McGraw-Hill Book Company, Inc., 1940.

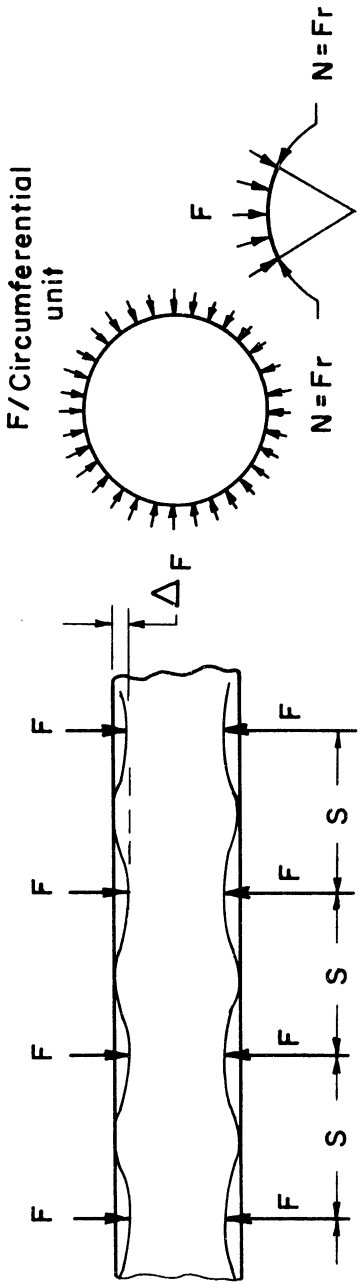

Figure 14. Infinitely Long Cylinder Subjected to Equally Spaced Radial Loads.

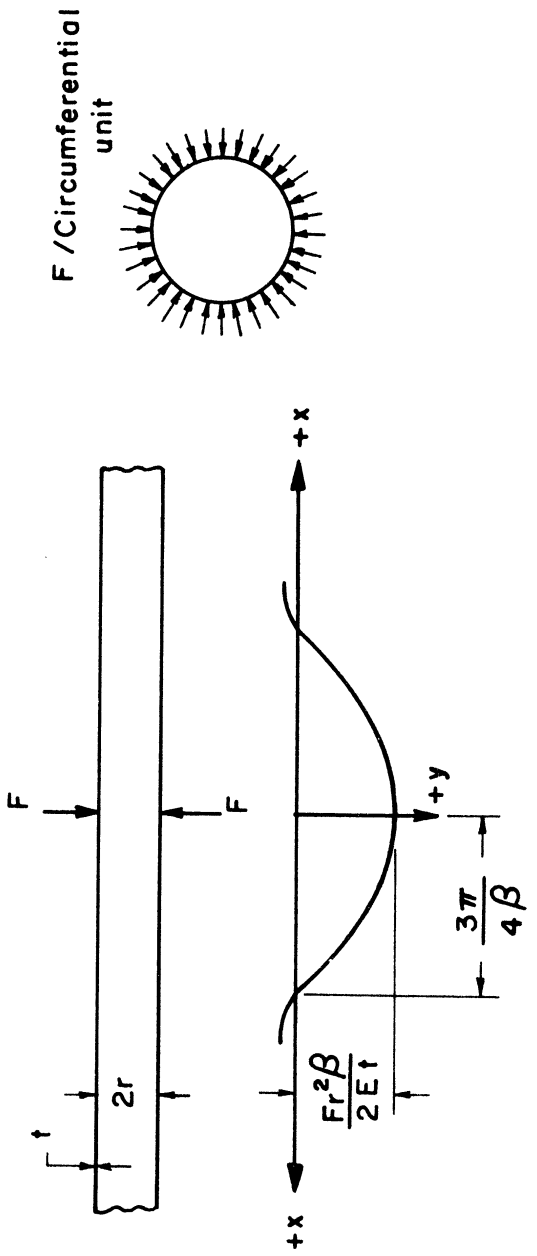

Figure 15. Infinitely Long Cylinder Subjected to Uniformly Distributed Radial Loading Along a Circular Section.

as has been defined by Equation (13)

$$\therefore \Delta_F = \frac{Fr^2\beta}{2Et} [\psi(\beta s)] \tag{20}$$

The tangential components of the forces "F" (Figure 14) can be written as:

$$N = Fr \quad \text{or} \quad F = \frac{N}{r}$$

The normal forces in the stiffener due to bulging of the cylinder are given in Equation (18). Therefore, the parameters governing the radial displacements in the cylinder at any stiffener location, due to the action of the stiffeners on the cylinder can be approximated by substituting N_r of Equation (18) for Fr of Equation (20). These radial displacements should be equal to the displacements in the cylinder due to bulging [given by Equation (17)], minus the radial displacements in the stiffener itself. This strain condition can be expressed by the following equation:

$$\frac{Zr \cos \phi \; r\beta}{2Et} [\psi (\beta s)] = \frac{\mu}{\pi r t} \frac{M}{E} \cos \phi - \frac{Zr^2}{AE} \cos \phi \tag{21}$$

(Note that $N_r = Zr \cos \phi$ of Equation (18) was substituted for (Fr) of of Equation (20). Also that r_r is taken equal to r.) Solving for Z of Equation (21), one obtains:

$$Z = \frac{\frac{\mu M}{\pi r^3}}{\frac{\beta}{2} [\psi(\beta s)] + \frac{t}{A_r}} \tag{22}$$

It should be noted here that the purpose of using the results of another problem was to establish the major parameters relative to the magnitude of the forces acting on the stiffeners due to the bulging of

the cylinder. Z as given by Equation (22) should only be used to establish the parameters rather than the magnitude of the forces acting on the stiffener. Two constants can be introduced to define the magnitude of Z which will make it possible to express the value of Z in the form:

$$Z = \frac{\frac{\mu M}{\pi r^3}}{\frac{\beta_1}{2}\left[\psi(\beta_1 s)\right] + C_3 \frac{t}{A_r}} \tag{23}$$

where

$$\beta_1 = \frac{C_4}{\sqrt{rt}} \quad .$$

If the value of Z as given by Equation (23) is substituted in Equation (18), then the following expression for N_r will result:

$$N_r = \frac{\frac{\mu M}{\pi r^2}\cos \phi}{\frac{\beta_1}{2}\left[\psi(\beta_1 s)\right] + C_3 \frac{t}{A_r}} \tag{24}$$

where

N_r = normal forces in the ring,

t = thickness of the cylinder wall,

A_r = cross-sectional area of the stiffener,

$\beta_1 = \frac{C_4}{\sqrt{rt}}$

Values of $C_3 = 1.0$ and $C_4 = 0.7$ were established by using all available experimental data for the two sizes of stiffeners used.

According to Equation (24) the stresses in the stiffener, due to bulging, will vary linearly with the applied bending moment on the cylinder. This is verified by the experimental results as shown in Figure 16 where both the experimental and theoretical stress at the top of the stiffener (Point 1) are plotted relative to the stress when

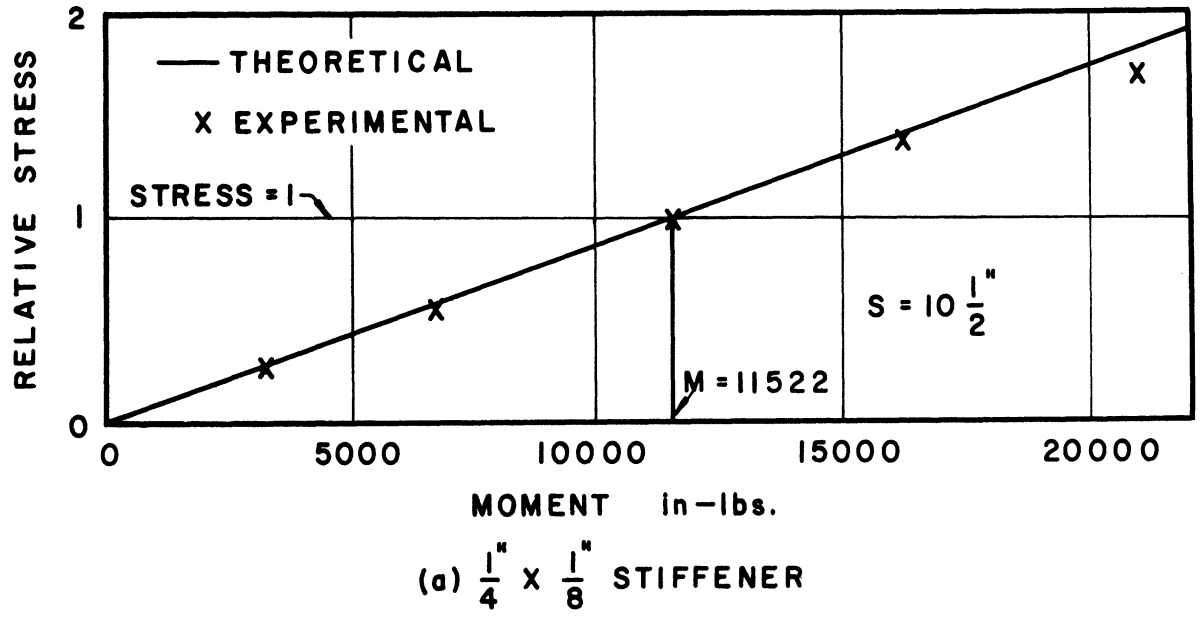

(a) $\frac{1}{4}$" X $\frac{1}{8}$" STIFFENER

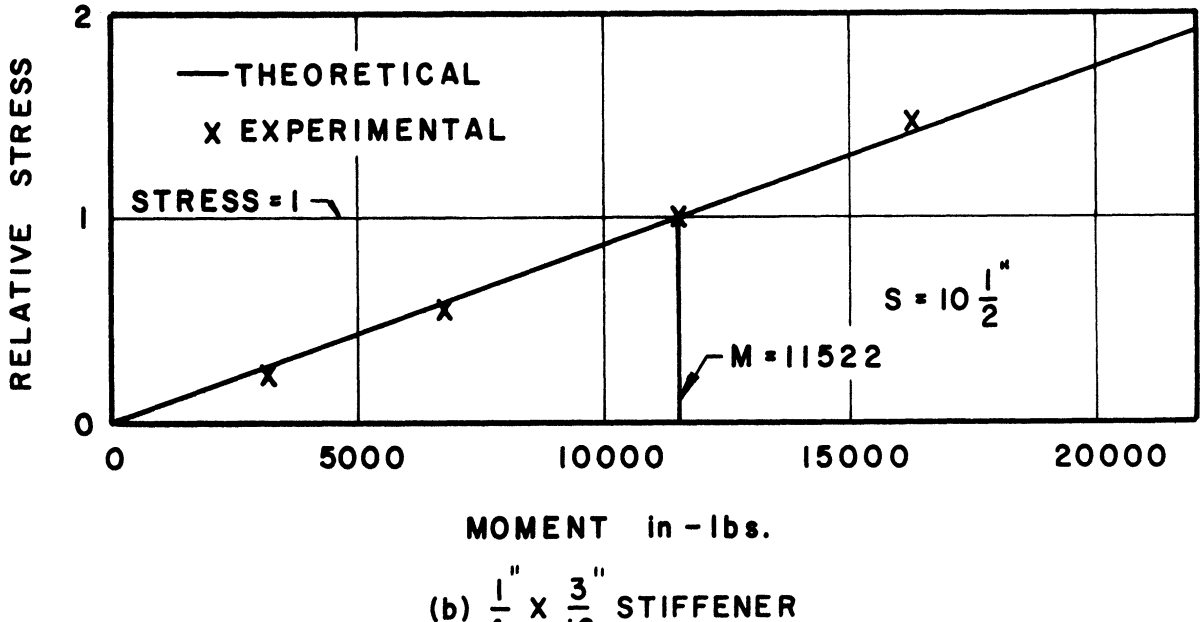

(b) $\frac{1}{4}$" X $\frac{3}{16}$" STIFFENER

Figure 16. Relative Stress vs. Moment (Bulging).

M = 11522 in-lbs. The stress at Point 1 when M = 11522 is taken to be equal to unity for both the theoretical and experimental values.

The variations of the stresses around the ring stiffener due to bulging should be proportional to cos ϕ. The comparison with the experimental results is shown in Figure 17. The discrepancy between the calculated and the experimental stresses can be attributed to the following:

(1) The distribution of the experimental stresses around the stiffener, due to the flattening effect, was assumed to be identical with the results of the analytical investigation. This means that all the experimental errors are carried over with the experimental stresses due to the bulging of the cylinder.

(2) The stresses in the stiffener due to bulging are computed on the basis of a certain distribution of forces acting on a perfectly circular section thus producing no bending moments in the stiffener. Any slight variations in the circular shape of the stiffener or in the distribution of the forces can produce bending moments in the stiffener which will result in appreciable changes in the stress.

The variations of the stresses in the stiffener due to the bulging of the cylinder are given in Figure 18 as a function of the spacing of the stiffeners. The reasonably good agreement between the calculated and the experimental stresses justified the general form of Equation (24).

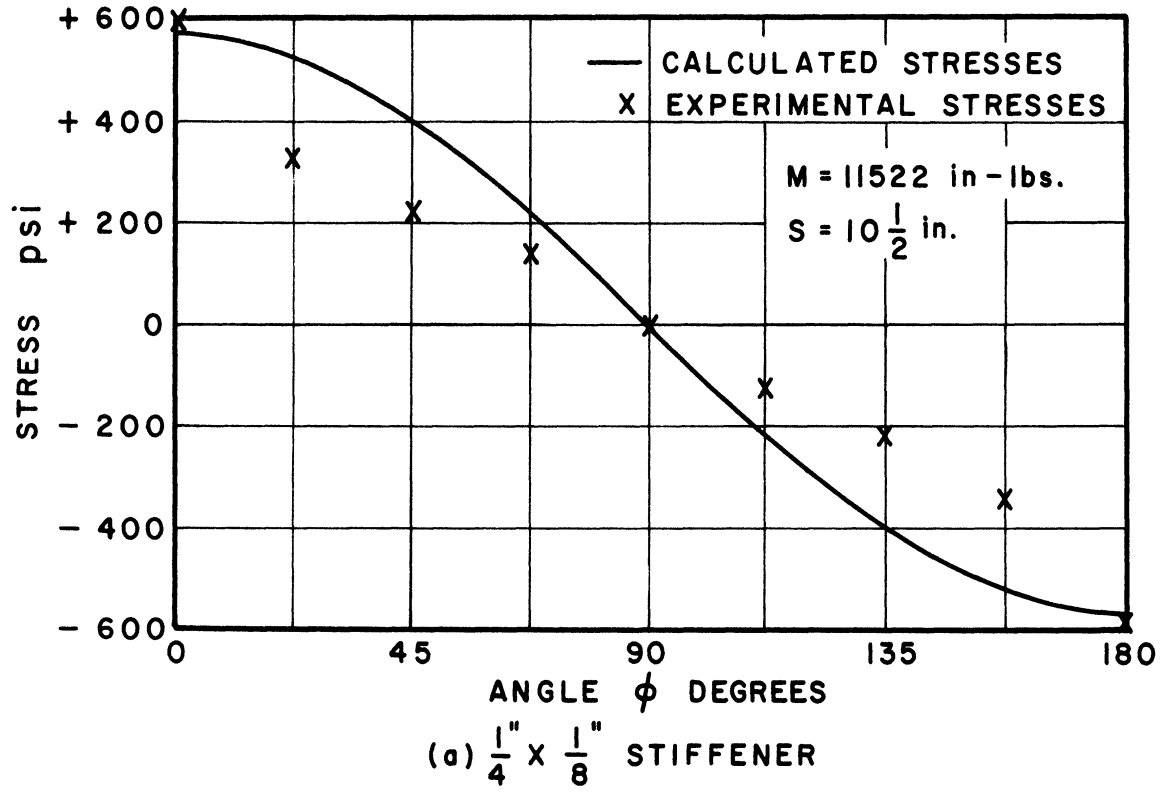

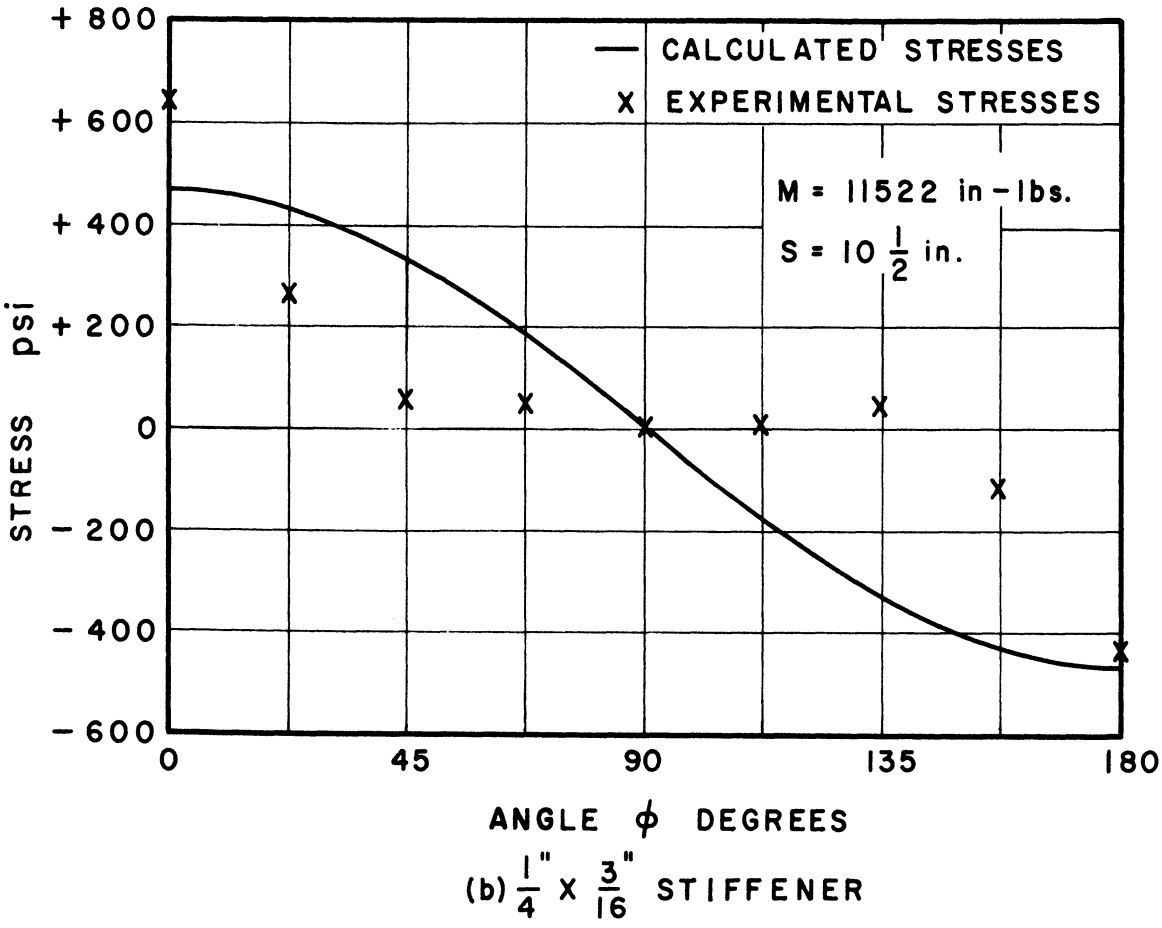

Figure 17. Variation of the Stresses Around the Stiffener (Bulging).

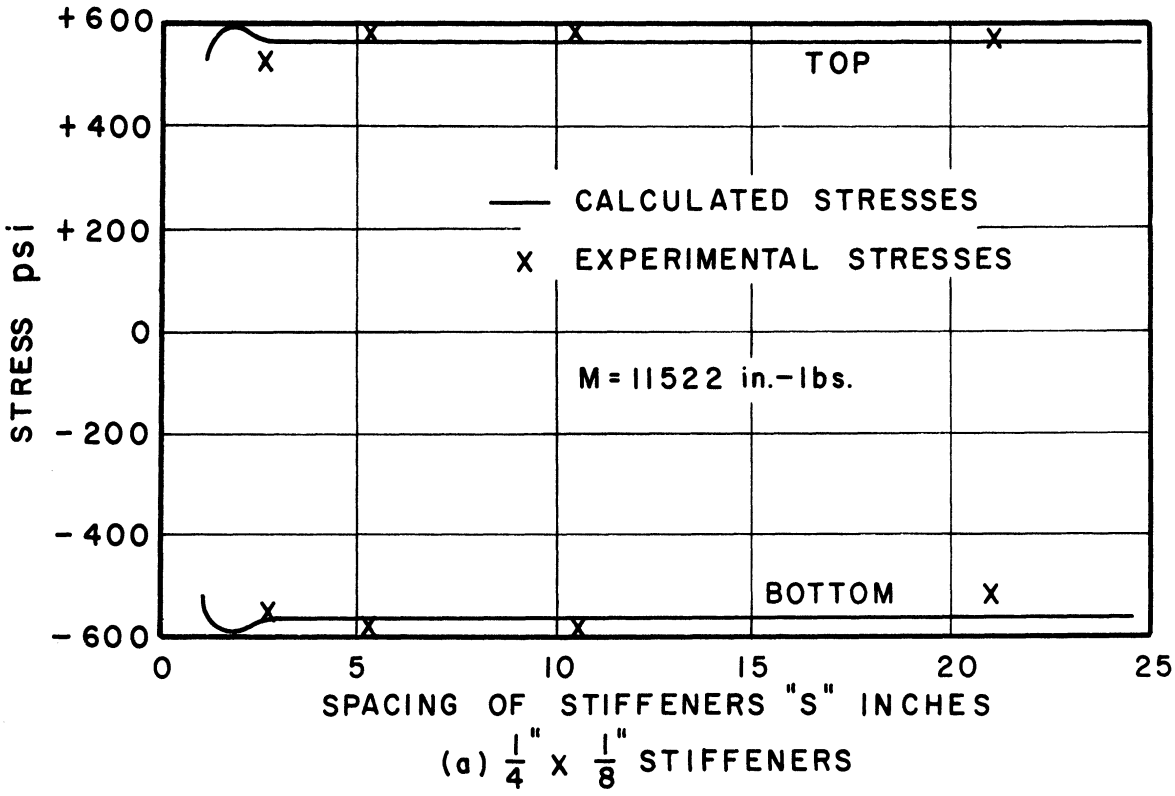

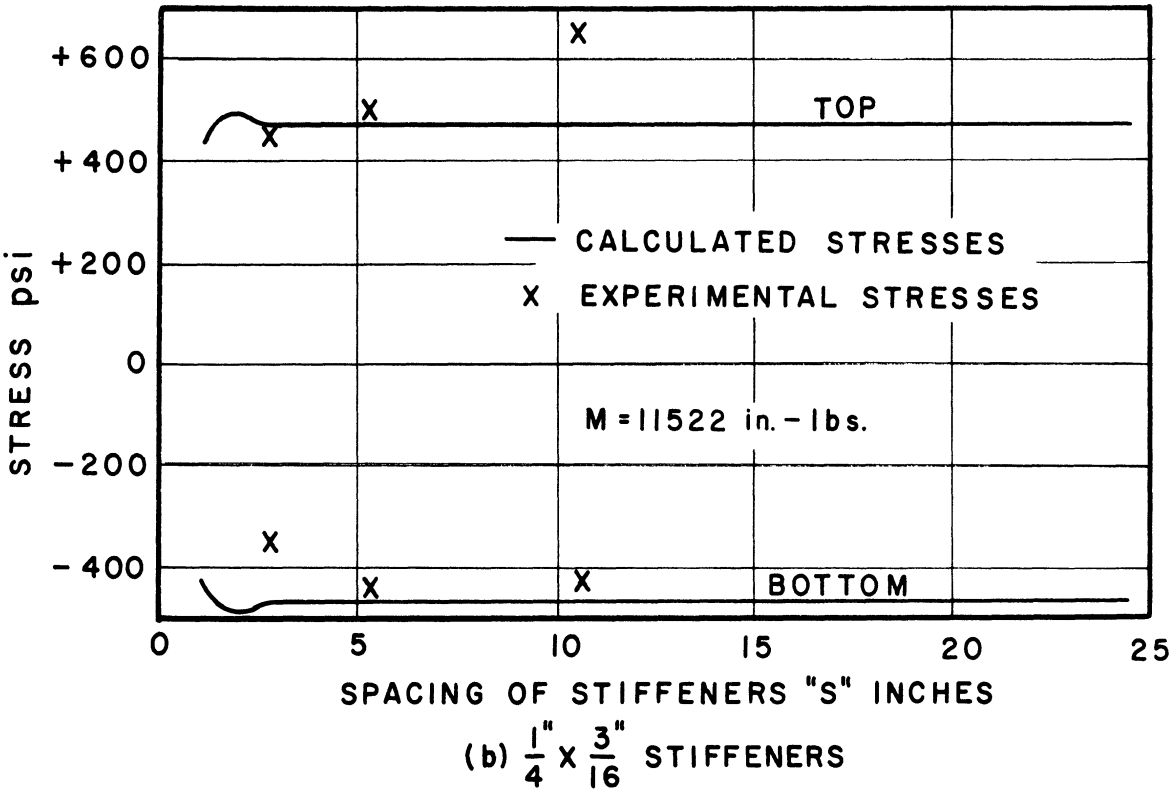

Figure 18. Stresses on the Outside Face of the Stiffener at the Top and Bottom vs. the Spacing of the Stiffeners (Bulging).

The Separate Effect of the Local Loading

The bending moments in the cylinder resulting from the application of any local loading will cause the cylinder to flatten and to bulge due to the general bending action of the cylinder. In addition to the flattening and to the bulging of the cylinder, the local loading will have a separate and an appreciable effect on the ring stiffeners.

If the cylinder is loaded by uniformly distributed radial loading on the top half, then the forces on the stiffeners, due to the separate effect of this loading, can be assumed to follow the distribution shown in Figure 19, where w is the magnitude of the radial pressure on the cylinder. The tangential forces of $\frac{2}{\pi} w' \sin \phi$ will satisfy the equilibrium condition. This distribution will be shown later to be justified by the experimental stresses.

The bending moments and the normal forces in the ring loaded as shown in Figure 19 are given by the following equations:

$$M_r = \left(\frac{1}{2} - \frac{3}{2\pi} \cos \phi - \frac{1}{\pi} \phi \sin \phi\right) w' r^2$$

$$\left[\text{For } 0 \leq \phi \leq \frac{\pi}{2}\right]$$

$$M_r = \left(\sin \phi - \frac{1}{2} - \frac{3}{2\pi} \cos \phi - \frac{1}{\pi} \phi \sin \phi\right) w' r^2 \qquad (25)$$

$$\left[\text{For } \frac{\pi}{2} \leq \phi \leq \pi\right]$$

$$N_r = \left(-\frac{1}{2\pi} \cos \phi - 1 + \frac{1}{\pi} \phi \sin \phi\right) w' r$$

$$\left[\text{For } 0 \leq \phi \leq \frac{\pi}{2}\right] \qquad (26)$$

$$N_r = \left(-\frac{1}{2\pi} \cos \phi - \sin \phi + \frac{1}{\pi} \phi \sin \phi\right) w' r$$

$$\left[\text{For } \frac{\pi}{2} \leq \phi \leq \pi\right]$$

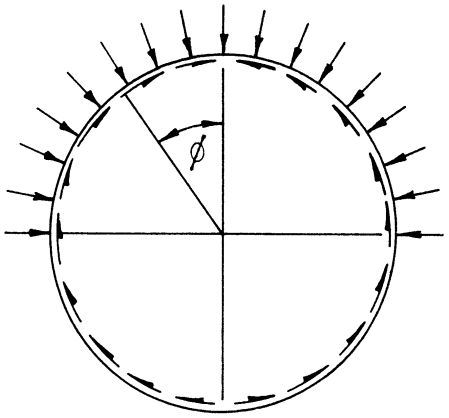

Figure 19. Forces on the Stiffener Due to the Separate Effect of Local Radial Loading.

In the above equations

$+M_r$ designates tension on the outside,

$+N_r$ designates tension

K' (Figure 19) which has the unit of length is a function varying with the spacing of the stiffeners and with the other parameters of the problem. The maximum value that K' can assume is S (spacing of the stiffeners) if the shell is assumed to be completely ineffective in resisting the local forces. A more accurate evaluation of K' can be obtained by assuming that K' has the same form as K of Equation (15), or:

$$K' = \frac{1}{\frac{\lambda'}{2}\left[\psi(\lambda' s)\right] + C_5 \frac{t^3}{I_r}} \qquad (27)$$

where

$$\lambda' = \frac{C_6}{r} .$$

The values of C_5 and C_6 that will best satisfy the experimental data were found to be equal to 0.21 and 0.45 respectively.

The stresses in the stiffener due to the separate effect of the local loading should vary linearly with the load according to Equations (25) and (26). The comparison with the experimental data is shown in Figure 20 where both the theoretical and experimental stresses at the top of the stiffener (Point 1) are plotted relative to the stress when W = 12-1/6 lbs. Both the theoretical and experimental stress are taken to be equal to unity when W = 12-1/6 lbs.

The variations of the stresses around the stiffener as a result of the separate effect of the local radial loading is given in

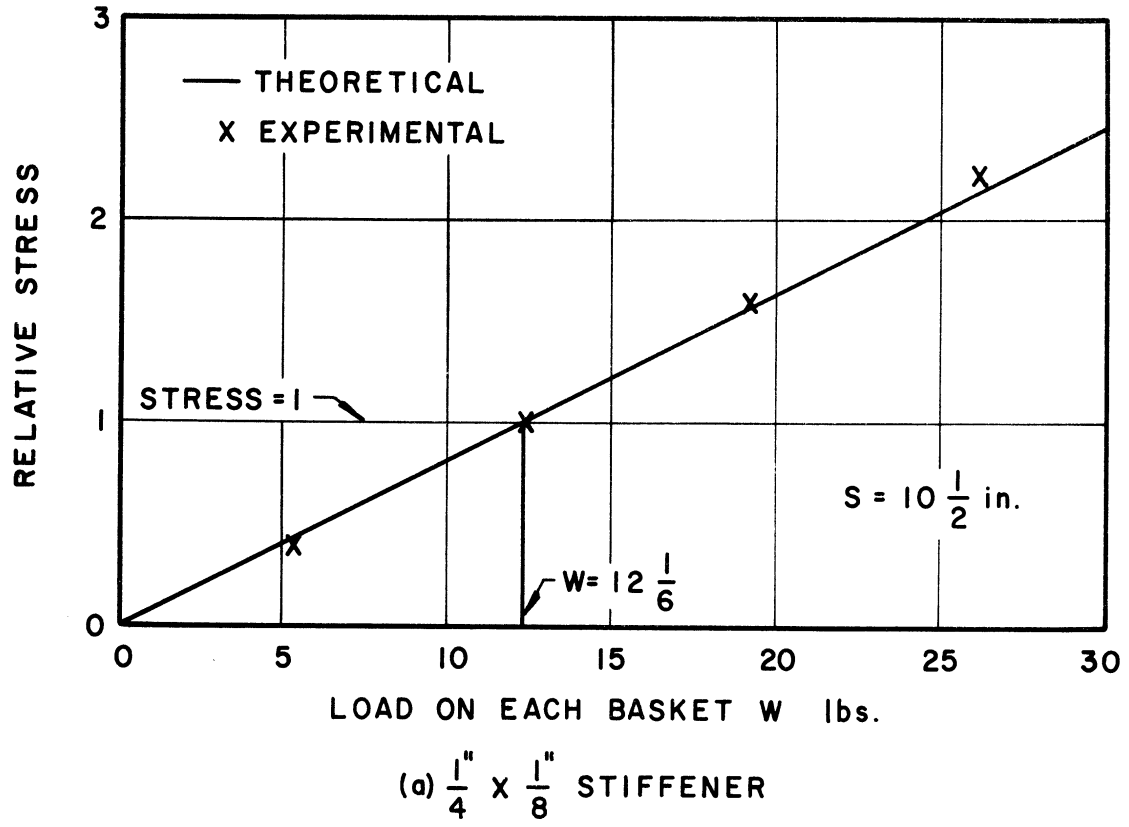

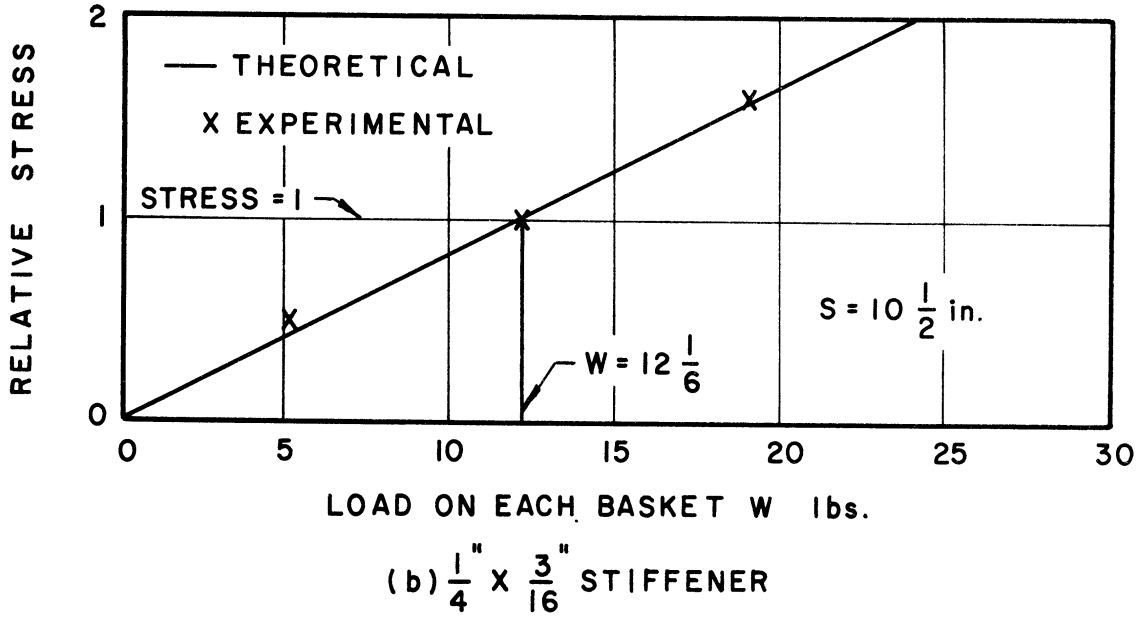

Figure 20. Relative Stress vs. Load. (Separate effect of the local loading)

Figure 21 for both calculated and measured stresses. It is important to mention here that the good agreement between the calculated and experimental stresses, insofar as the distribution of the stresses around the stiffener is concerned, justifies the assumed distribution of the forces of Figure 19.

Figure 22 shows the variations of the stresses in the stiffener due to the separate effect of the radial local loading, as a function of the spacing of the stiffeners. Both the calculated stresses and the experimental stresses are shown for the 1/4" x 1/8" stiffener at Points 1 and 9 (top and bottom of the stiffener). It should be noted that the values of C_5 and C_6 were chosen so that the best agreement was obtained between experimental and calculated stresses at both the top and the bottom of the stiffener. It is believed that the discrepancy between calculated and measured stresses is the result of assuming that the baskets transmitting the local loading on the cylinder produce uniform radial pressure on the top half of the shell. This assumption can be in error due mainly to the frictional forces between the bands and the shell. It is interesting to observe the better agreement between calculated and measured stresses on the bottom half of the stiffener (see Figure 21).

CONCLUSIONS

The three types of action that are discussed in this paper, namely: the flattening, the bulging and the separate effect of the local loading, are considered to be the major factors in determining

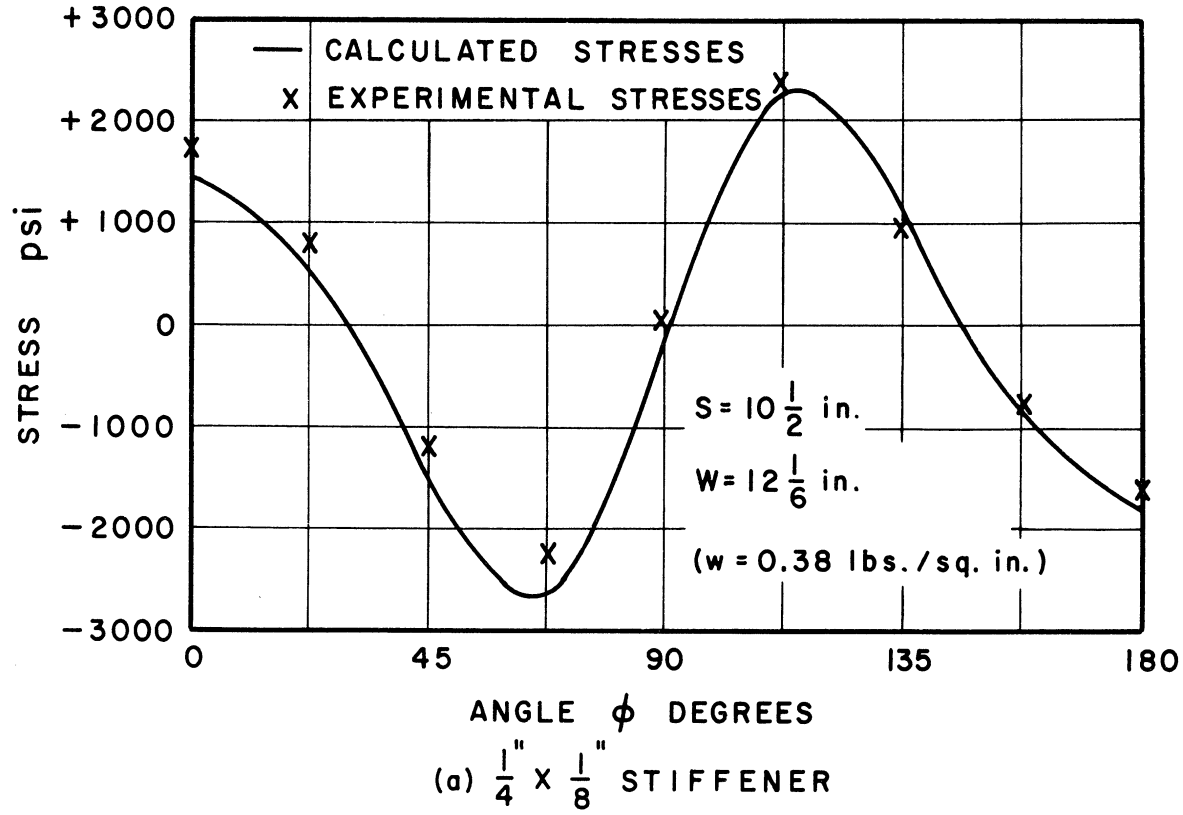

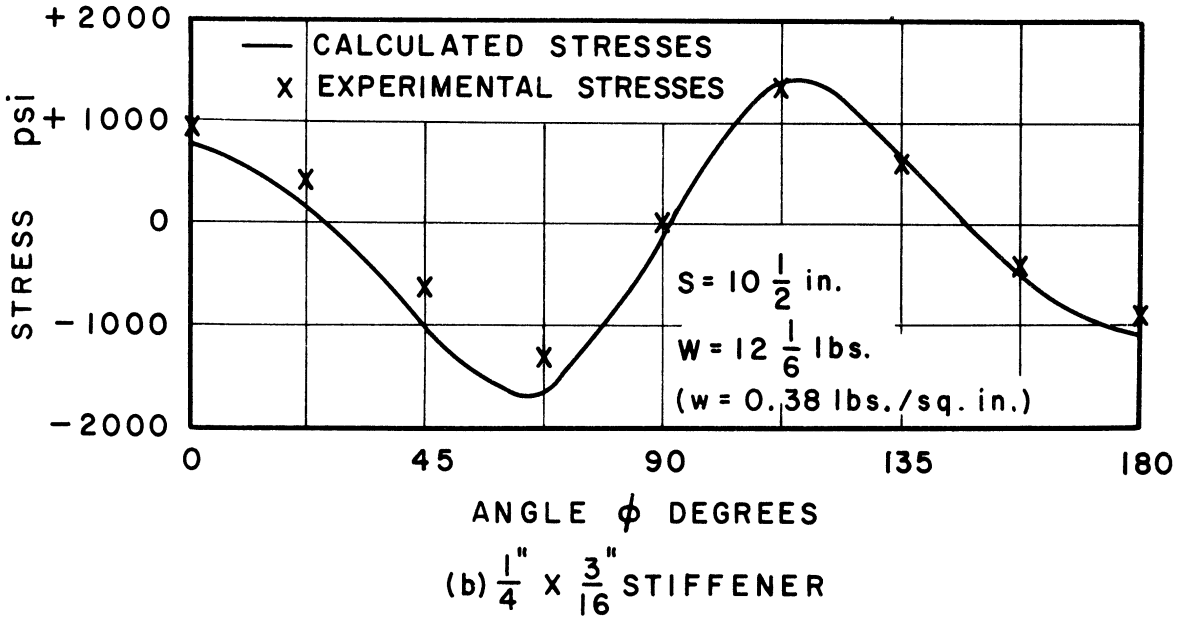

Figure 21. Variation of the Stresses Around the Stiffener. (Separate effect of the local loading.)

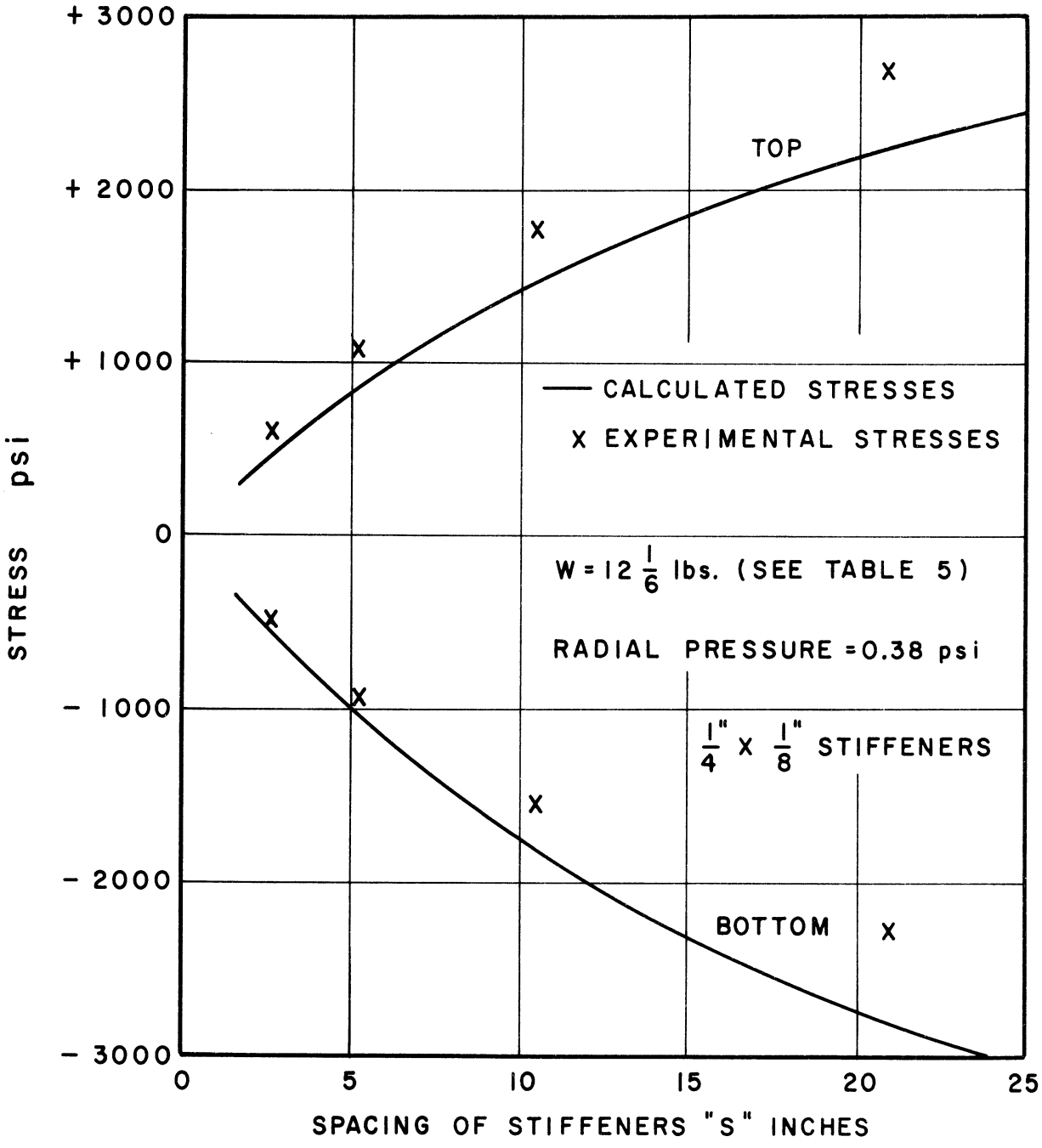

Figure 22. Stresses on the Outside Face of the Stiffener at Top and Bottom vs. the Spacing of the Stiffeners. (Separate effect of the local loading.)

the forces acting on ring stiffeners in long thin-walled cylinders subjected to bending.

For each type of action the assumed forces on the stiffener resulted in a distribution of stresses around the stiffener which were shown to agree reasonably well with the experimental results.

It can be stated, therefore, that the stresses in the ring stiffeners can be safely computed by the formulas developed in this paper. The bending moments and the normal forces due to flattening can be computed by Equations (3), (4) and (15) while the normal forces due to bulging can be computed by Equation (24). From the limited experimental results, values of $C_1 = 1.0$, $C_2 = 1.1$, $C_3 = 1.0$ and $C_4 = 0.7$ are recommended for use in conjunction with the above equations.

The moments and normal forces in the rings due to the separate effect of the local loading will depend upon the distribution of the local forces on the cylinder. To illustrate this type of action, one particular kind of local loading was investigated.

The maximum stresses in the rings can then be obtained by a combination of the above three actions.

ACKNOWLEDGMENT

This investigation is based on the author's doctoral thesis[6] at the University of Michigan, submitted to a doctoral committee under the chairmanship of Professor Lawrence C. Maugh.

---

[6] Rumman, W. S. An Experimental Study of the Stresses in Ring Stiffeners in Long Thin-Walled Cylinders Subjected to Bending. Ph.D. Dissertation, The University of Michigan, 1959.

APPENDIX I

NOMENCLATURE

A_r	Cross sectional area of the ring stiffener
E	Modulus of Elasticity
I_r	Moment of Inertia of the ring stiffener
M	Applied moment on the cylinder
M_r	Bending moment in the ring stiffener
N_r	Normal force in the ring stiffener
r	Mean radius of the cylinder
S,s	Spacing of the ring stiffeners
t	Wall thickness of the cylinder
W	Weight on each loading basket (see Table II)
w	Uniformly distributed radial loading on the top half of the cylinder
μ	Poisson's ratio
ρ	Radius of curvature of the cylinder
σ	Stress

Other symbols are defined throughout the text.

APPENDIX II

VALUES OF THE FUNCTION

$$\psi(x) = 1 + 2 \sum_{n=1}^{\infty} e^{-nx} (\cos nx + \sin nx)$$

x	$\psi(x)$	x	$\psi(x)$	x	$\psi(x)$
0.10	20.002	1.40	1.459	3.40	0.921
0.20	10.001	1.50	1.370	3.60	0.929
0.30	6.667	1.60	1.295	3.80	0.938
0.40	5.001	1.70	1.230	4.00	0.949
0.50	4.002	1.80	1.174	4.50	0.973
0.60	3.336	1.90	1.127	5.00	0.991
0.70	2.861	2.00	1.086	5.50	1.000
0.80	2.506	2.20	1.021	6.00	1.003
0.90	2.230	2.40	0.976	6.50	1.004
1.00	2.011	2.60	0.945	7.00	1.003
1.10	1.833	2.80	0.927	7.50	1.001
1.20	1.686	3.00	0.919	8.00	1.001
1.30	1.563	3.20	0.917		